Research article

JGS
Journal of the Geological Society

https://doi.org/10.1144/jgs2020-183 | Vol. 178 | 2021 | jgs2020-183

Pre-Zanclean end of the Messinian Salinity Crisis: new evidence from central Mediterranean reference sections

Speranta-Maria Popescu[1*], William Cavazza[2], Jean-Pierre Suc[3], Mihaela Carmen Melinte-Dobrinescu[4], Nadia Barhoun[5] and Christian Gorini[3]

[1] GeoBioStratData.Consulting, 385 Route du Mas Rillier, 69140 Rillieux la Pape, France
[2] Department of Biological, Geological and Environmental Sciences, University of Bologna, Piazza di Porta San Donato 1, 40126 Bologna, Italy
[3] Sorbonne Université, CNRS-INSU, Institut des Sciences de la Terre Paris, ISTeP UMR 7193, 75005 Paris, France
[4] National Institute of Marine Geology and Geo-Ecology, 23–25 Dimitrie Onciul Street, 70318 Bucharest, Romania
[5] University Hassan II of Casablanca, Faculty of Sciences Ben M'Sik, BP7955 Sidi Othmane, Casablanca, Morocco
S-MP, 0000-0001-5345-395X; WC, 0000-0002-6030-9689; J-PS, 0000-0002-5207-8622; MCM-D, 0000-0003-4716-6844; NB, 0000-0002-0112-4318; CG, 0000-0003-3123-4822
* Correspondence: speranta.popescu@gmail.com

Abstract: The concept of a geologically instantaneous earliest Zanclean reflooding of the Mediterranean Basin after the Messinian drawdown has dominated geological thinking and is ingrained in the scientific literature. The base of the Trubi Formation in southern Italy, formally defined as the Zanclean Global Boundary Stratotype Section and Point (GSSP) at 5.33 Ma, has traditionally been considered as marking the marine reflooding of the Mediterranean. However, several studies provide evidence that marine reflooding occurred prior to the Zanclean GSSP, the most reliable of which comes from southern Calabria. Here, we show that the sedimentary coastal prism cropping out extensively immediately below the base of the Trubi Formation in this region and correlatable with the Arenazzolo Unit in Sicily contains a fully marine micropalaeontological association of calcareous nannofossils and dinoflagellate cysts, thus pointing to both a high sea-level and marine conditions before deposition of the Trubi Formation (i.e. in the latest Messinian).

Received 24 September 2020; **revised** 8 January 2021; **accepted** 18 January 2021

The Mediterranean Messinian Salinity Crisis (MSC) (Selli 1954; Hsü *et al.* 1973*a*) was an extraordinary event as it has been estimated that 5% of the dissolved salt of the global ocean precipitated in a few hundred thousand years to form a deposit with a volume of more than 1×10^6 km^3 (Ryan 2009) with considerable effects on global atmospheric, oceanographic and climatic patterns (e.g. Adams *et al.* 1977; Thunnell *et al.* 1987; Sternai *et al.* 2017). After sporadic pioneering work both on land (e.g. Ogniben 1957; Selli 1960; Decima 1964; Ruggieri 1967) and offshore (e.g. Glangeaud *et al.* 1966; Montadert *et al.* 1970), the MSC attracted considerable attention when Deep Sea Drilling Project (DSDP) Leg 13 drilled the top of the evaporites in several western Mediterranean sites and confirmed the existence of an extensive volume of Messinian evaporites (Hsü 1972; Hsü *et al.* 1973*a*, *b*). Since DSDP Leg 13, the MSC has been the focus of extensive research resulting in an intense international debate mainly focused on its process, timing and consequences.

The MSC is now envisioned as a two-step process (Clauzon *et al.* 1996), a scenario largely accepted by the scientific community (CIESM 2008; Roveri *et al.* 2014). The first step affected the Mediterranean peripheral basins (including Sicily) and is characterized by thick deposits of evaporites owing to a drop of about 150 m in the Mediterranean sea-level. The second step affected the Mediterranean central basins where thick evaporites were deposited as a result of the sea-level drawdown of about 1500 m, which also caused intense subaerial erosion of the margins, mainly by the rivers.

The specialized community unanimously agrees on a chronology ranging from 5.97 to 5.60 Ma for the first step of the MSC (Gautier *et al.* 1994; Krijgsman *et al.* 1999, 2001; Manzi *et al.* 2013). There is a wide agreement about the age of the onset of the paroxysmic second step of the MSC at 5.60 Ma. The end of the MSC, which corresponds to the sudden reflooding of the Mediterranean Basin by Atlantic waters, is usually dated at 5.33 Ma; that is, the age of the base of the Trubi Formation (Zanclean Global Boundary Stratotype Section and Point (GSSP)) established both in Sicily and in southern Calabria (Channell *et al.* 1988; Hilgen and Langereis 1993; Van Couvering *et al.* 2000). The proposal by Brolsma (1975, 1976) that marine reflooding occurred prior to the Zanclean (i.e. at the base of the Arenazzolo deposits underlying the Trubi Formation) introduced the first doubts concerning the robustness of the reflooding age at 5.33 Ma. Later, several studies provided evidence that marine conditions existed on the Mediterranean margins prior to the beginning of the Zanclean (Cavazza and DeCelles 1998; Londeix *et al.* 2007; Carnevale *et al.* 2008; Bache *et al.* 2012; Pellen *et al.* 2017), a context that was considered likely by Riding *et al.* (1998), Aguirre and Sánchez-Almazo (2004), Cornée *et al.* (2006), Soria *et al.* (2008), Melinte-Dobrinescu *et al.* (2009), Do Couto *et al.* (2014) and Clauzon *et al.* (2015) despite the absence of conclusive relationships with the formal basal Zanclean. According to Bache *et al.* (2012, 2015), the continuous input of Atlantic waters in the almost desiccated Mediterranean central basins started during the late Messinian (at *c.* 5.55 Ma) and ended with the sudden and dramatic reflooding estimated at 5.46 Ma. The presence of marine microplankton in the drilled uppermost part of the central evaporites (second step of the MSC) has long been known (Cita 1973; Cita *et al.* 1978; Iaccarino and Bossio 1999) although its reliability is still under discussion (Popescu *et al.* 2015). Marine reflooding of the Mediterranean Basin is interpreted as occurring at either 5.46 Ma (Bache *et al.* 2015; Clauzon *et al.* 2015; Popescu *et al.* 2015; Suc *et al.* 2015) or 5.33 Ma (Roveri *et al.* 2014; Krijgsman *et al.* 2018). Although not directly linked with the

purpose of this paper, but closely associated with the reference sections in Sicily, the continuing debate concerning Lago Mare (LM) needs clarifying: characterized by the occurrence of Paratethyan species in the Mediterranean, one episode is considered as closing the MSC (Roveri *et al.* 2014) and three distinct episodes have been chronologically distinguished by Clauzon *et al.* (2005) and Popescu *et al.* (2015).

Southern Calabria provides the most robust evidence of a pre-Zanclean coastal sedimentary prism (DeCelles and Cavazza 1992, 1995; Cavazza and DeCelles 1998), exposed immediately below the Trubi Formation in the areas of Monte Singa (Zijderveld *et al.* 1986; Hilgen 1987, 1991; Hilgen and Langereis 1993) and Capo Spartivento (Channell *et al.* 1988), which are among the reference sections for the establishment at Eraclea Minoa of the Miocene–Pliocene boundary (Van Couvering *et al.* 2000). Our target was to find marine microfossils (possibly biostratigraphic markers) within the Calabrian coastal prism underlying the formal Lower Pliocene, with the aim of proving that the Mediterranean reflooding occurred significantly before the earliest Zanclean.

Geological framework

The Calabria–Peloritani Terrane (CPT) is an exotic terrane composed of several nappes piled up during Alpine-age deformation and involving an ancient crystalline basement affected by the Hercynian orogeny (Amodio Morelli *et al.* 1976; Bonardi *et al.* 2001). Although originally part of the European southern continental margin, the CPT rifted off the margin in the Oligocene after the Alpine collision and drifted southeastward during the Neogene until it collided with the African continental margin in Langhian (early Middle Miocene) time (Alvarez *et al.* 1974; Dercourt *et al.* 1985; Malinverno and Ryan 1986; Dewey *et al.* 1989; Gueguen *et al.* 1998; Jolivet and Faccenna 2000; Cavazza *et al.* 2004). The Ionian coast of southeastern Calabria is arguably the only place in western and central Mediterranean regions where an Alpine-age continental collision has not occurred. In this region, northwestward subduction of the Ionian Neotethyan oceanic lithosphere is still under way, albeit passively, under the Calabrian microplate, as indicated by a northwestward dipping subduction plane (e.g. Spakman and Wortel 2004) and by the mostly Quaternary calcalkaline volcanism of the Aeolian Islands (e.g. De Astis *et al.* 2003).

The Ionian forearc basin is located between the subduction zone and the CPT basement units cropping out on land (Fig. 1b and c). The term ‘forearc’ is used here to define the location of the basin between the Ionian subduction zone and the corresponding calcalkaline volcanic arc of the Aeolian Islands, with no implications as to the mechanism responsible for the development of the basin. The proximal portion of the Ionian forearc basin fill crops out extensively along the southeastern coast of Calabria owing to rapid uplift of the CPT since the Middle Pleistocene (Tortorici *et al.* 1995). This uplift has been interpreted as resulting from unflexing of

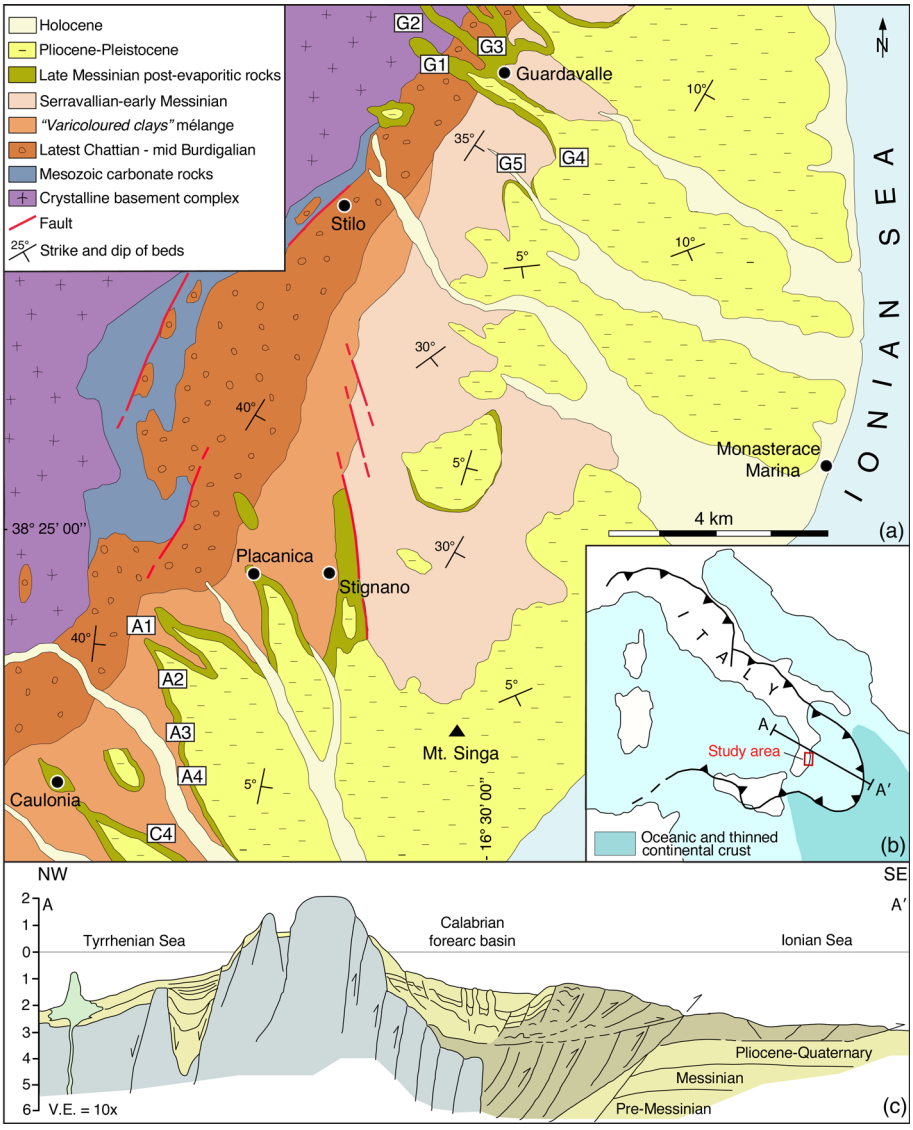

Fig. 1. (**a**) Simplified geological map of the study area (after Cavazza and DeCelles 1998). Labels indicate location of stratigraphic sections shown in Figures 5 and 6. (**b**) Present-day geodynamic sketch of the central Mediterranean region. (**c**) Structural cross-section across the Calabrian orogenic wedge and forearc basin (from Van Dijk 1992, modified). (See (**b**) for location of cross-section.)

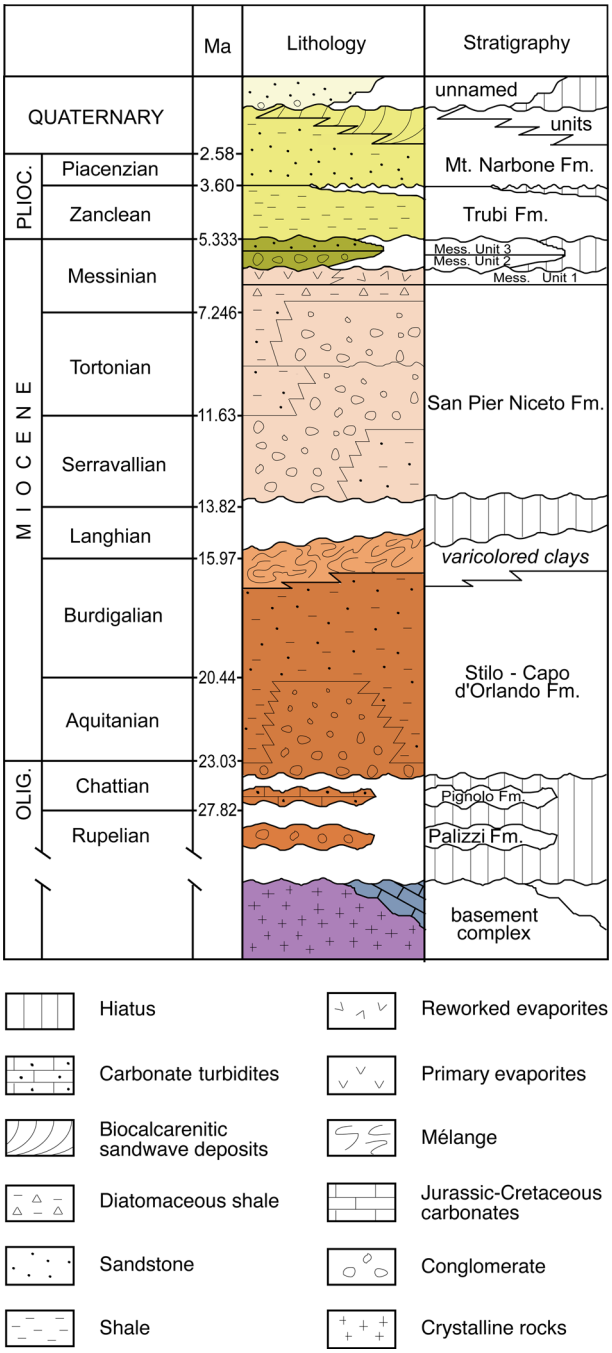

Fig. 2. Chronolithostratigraphy of the Ionian forearc-basin fill in southeastern Calabria. Sources: DeCelles and Cavazza (1992, 1995); Cavazza and DeCelles (1993, 1998); Patterson *et al.* (1995); Cavazza *et al.* (1997); Bonardi *et al.* (2001); Cavazza and Barone (2010); and unpublished data. Timescale after Cohen *et al.* (2020).

the Ionian foreland lithosphere upon break-off of its subducted slab following the docking of the CPT (e.g. Spakman and Wortel 2004).

Along the Ionian coast of southeastern Calabria, the proximal portion of the forearc basin fill is >2000 m thick and comprises upper Oligocene to Quaternary lithostratigraphic units (Figs 2 and 3) (Cavazza *et al.* 1997; Bonardi *et al.* 2001), with an overall upward-shallowing trend. The basal part of the basin fill is formed by uppermost Chattian–Burdigalian turbidite deposits of the Stilo–Capo d'Orlando Formation (Bonardi *et al.* 1980; Cavazza 1989; Cavazza and DeCelles 1993) conformably overlain by a large-scale olistostrome mélange informally named Varicoloured clays (Cavazza and Barone 2010). The latter is overlain by the San Pier Niceto Formation, a Serravallian–Tortonian succession of proximal marine conglomerate, sandstone and mudstone (Critelli et al. 2015*a*, *b*). The Messinian stratigraphy is described in more detail below. The carbonate–marl rhythms of the Zanclean Trubi Formation onlap all the older lithostratigraphic units and are, in turn, overlain by Upper Pliocene–Lower Pleistocene shallow marine calcarenite, siliciclastic sandstone and mudstone. Beach and fluvial terraces discontinuously cover older formations and can be found at elevations more than 1000 m above sea-level, indicating a dramatic uplift of the Calabrian block during the last 700 kyr (e.g. Tortorici *et al.* 1995).

Messinian physical stratigraphy and sedimentological facies

This section mostly refers to previously published data (DeCelles and Cavazza 1992; Cavazza and DeCelles 1998), which are briefly summarized here. The Messinian evaporitic and post-evaporitic succession that crops out along the Ionian coast of southeastern Calabria comprises three units (Figs 2 and 3). Lower Messinian evaporites and pelites (Unit 1) are conformable or slightly unconformable with respect to the underlying units, whereas the upper Messinian siliciclastic deposits (units 2 and 3) are mainly subhorizontal, essentially undeformed, and are separated from the underlying succession by an angular unconformity or a laterally equivalent disconformity. Some of the more complete outcrops of the Messinian post-evaporitic succession are located between the towns of Guardavalle to the north and Caulonia to the south (Fig. 1). In the present study, we mainly focused on such outcrops but also conducted observations on the Messinian stratigraphy over *c.* 80 km along depositional strike.

The limestone–gypsum succession of Unit 1

Unit 1 (Formazione di Cattolica of Critelli *et al.* 2015*a*, *b*) consists of a thin discontinuous limestone–gypsum succession conformably overlying the Serravallian–Tortonian succession of the San Pier Niceto Formation and the lowermost, pre-evaporitic Messinian (Figs 3 and 4). The maximum total thickness of Unit 1 is *c.* 100 m. In the study area, the limestone member (known elsewhere as Calcare di Base; Ogniben 1957) is largely recrystallized, and its original fabric is difficult to recognize. It is composed of micritic–microsparitic aggregates, probably pseudo-oolites related to algal activity (see Decima *et al.* 1988), or fecal pellets, set in microsparitic cement. In other areas, this lithostratigraphic unit comprises abundant filament-like peloids, arguably owing to the activity of cyanobacteria (Guido *et al.* 2007) similar to those described in the Messinian evaporites by Vai and Ricci-Lucchi (1977) and Manzi *et al.* (2011). Thin layers of macro- and mesocrystalline gypsum with swallowtail twinning are occasionally present within the limestone. The gypsum member of Unit 1 discontinuously overlies the limestone member described above. It is made of epiclastic gypsum-arenite and gypsum-rudite; no primary gypsum was found.

The fanglomerates of Unit 2

Unit 2 (Formazione di Monte Canolo of Critelli *et al.* 2015*a*, *b*) is up to 80 m thick and thins progressively southeastward (Fig. 5) or southward (Fig. 6) to <10 m, although the actual pinch-out is not visible. It consists of poorly to medium sorted cobble to boulder conglomerate. Average maximum clast size in individual beds ranges from 15 to 160 cm; no clear vertical trends in grain-size are visible although the bulk of Unit 2 fines systematically eastward. The most common conglomerate lithofacies are generally clast supported and comprise horizontally stratified, imbricated and structureless conglomerate. At a larger scale, the bedding is crudely lenticular. Imbrications indicate south-southeastward palaeoflow.

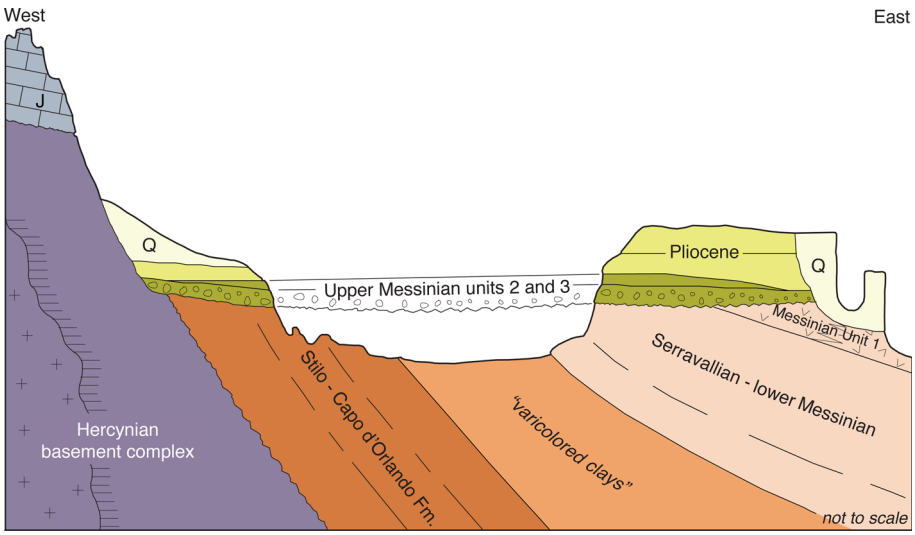

Fig. 3. Overall geometric relationships between the various lithostratigraphic units cropping out in the study area. The sketch is not to be intended as an actual geological section across any given area but as a broad depiction of the geometric relationships valid over the entire region. A noteworthy feature is the sharp intra-Messinian angular unconformity between the early Messinian evaporites (Unit 1) and the overlying late Messinian post-evaporitic fanglomerates (Unit 2) and sandstone-dominated coastal deposits (Unit 3). Messinian Unit 3 pinches out toward both the continent and the Ionian Basin, thus defining a sedimentary prism, and it is overlain by the Early Pliocene Trubi Formation.

Unit 2 is interpreted as deposits of stream-dominated alluvial fans (Cavazza and DeCelles 1998). Conglomerate clast composition is dominated by plutonic and subordinate phyllitic rocks, with small amounts (<5%) of Mesozoic and Lower Cenozoic carbonates. Taken together, compositional and palaeocurrent data indicate that the upper Messinian fanglomerates of Unit 2 were derived from the Hercynian basement complex directly to the WNW of the study area.

The sedimentary prism of Unit 3

The thickness of Unit 3 in the outcrops ranges from 0 to 52 m. In the Guardavalle fence diagram (Fig. 5), Unit 3 pinches out southeastward, whereas in the Caulonia fence diagram, it can be seen pinching out northwestward and its eastward continuation lies in the subsurface (Fig. 6). Based on stratigraphic or sedimentological measurements and field observations, this unit has a ribbon geometry elongated along the strike of the latest Messinian depositional system and nearly parallel to the present-day coastline. Based on geometric considerations, the width of Unit 3 perpendicular to depositional strike is estimated to be 3–4 km. A variety of sedimentological facies and facies associations are observed in Unit 3 (e.g. Figs 7 and 8). The following is a concise description; interested readers should refer to DeCelles and Cavazza (1992) and Cavazza and DeCelles (1998) for details.

The stratigraphy of Unit 3 is characterized by poorly cemented, very fine- to coarse-grained sandstone arranged in vertically coherent sequences typically consisting of structureless medium- to coarse-

Fig. 4. The intra-Messinian unconformity at Careri. Messinian evaporite beds of Unit 1 (dashed lines) are unconformably overlain by subhorizontal fanglomerate beds of upper Messinian Unit 2.

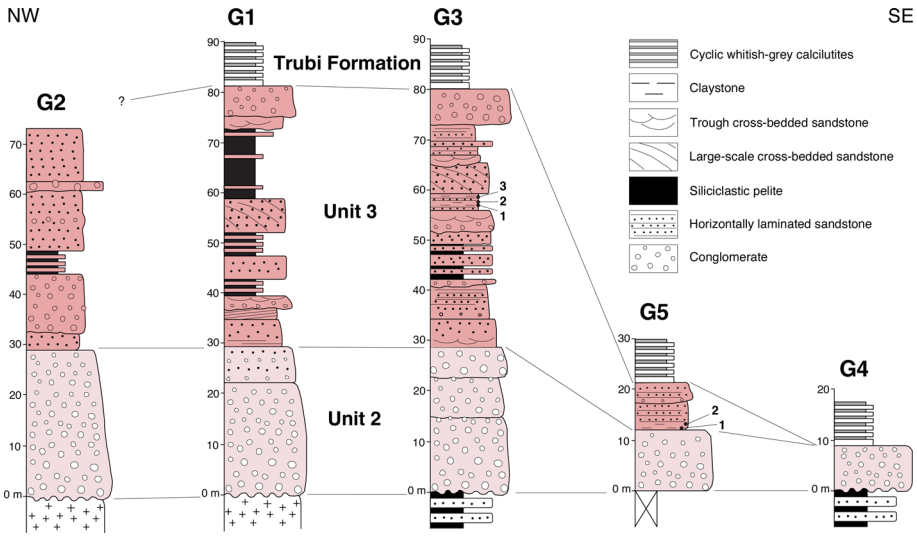

Fig. 5. Stratigraphic diagram of the upper Messinian post-evaporitic units of the Guardavalle region. G1–G5 are the studied sections with the number and place of the analysed samples indicated by black dots (see Fig. 1 for location). Evaporites (Unit 1 of Figs 2 and 3) are absent in this region. Coarse-grained upper Messinian fanglomerates (Unit 2) overlie unconformably either the crystalline basement complex (columns G1 and G2) or sedimentary deposits of Serravallian–Tortonian age (columns G3 and G4). Upper Messinian shallow marine to transitional deposits of Unit 3 define a sedimentary prism pinching out toward the SE. Columns G1–G4 after Cavazza and DeCelles (1998).

grained sandstone, overlain by medium- to coarse-grained trough cross-stratified and hummocky cross-stratified sandstone, in turn overlain by low-angle, laminated, very well sorted sandstone (e.g. Fig. 7). An irregular erosional surface, overlain by coarse-grained trough cross-stratified sandstone or imbricated pebble conglomerate, forms the upper part of a few of these sequences. These recurring sequences have been interpreted as progradational shallow marine to fluvial parasequences (DeCelles and Cavazza 1992; Cavazza and DeCelles 1998). The shallow marine parts of these sequences consist of a storm-dominated surf zone, beach and beach-ridge deposits. Where present, the beach-ridge deposits show large-scale, low-angle, bidirectional cross-stratification, and are associated with interlayered claystone and siltstone (or very fine-grained sandstone) with flaser bedding, starved ripples and wavy lamination. This association of finer grained lithofacies has been interpreted as the deposits of shallow lagoons on the landward sides of beach ridges (DeCelles and Cavazza 1992; Cavazza and DeCelles 1998).

Overall, the Messinian sediments of Unit 3 in eastern Calabria were deposited along an east-facing shoreline rather resembling the modern shoreline, where ephemeral gravelly braided streams drain the nearby highlands and form small braid-delta systems along an otherwise straight and open shoreface dominated by storm-wave-driven currents and negligible tidal processes. Spits parallel to the shore occasionally separate the alongshore deflected fluvial channels from the open shoreface and shallow lagoons develop where fluvial channels are abandoned. Locally, a thin dark clayey bed caps Unit 3 deposits (sections A2, A4 and C4; Fig 6), in sharp colour contrast to the immediately overlying white first carbonate bed of the Trubi Formation. The interpretation of this distinctive bed, shown in the sections of Figure 6, is proposed below.

Overall interpretation of Messinian stratigraphy

Despite local erosional features, the evaporites of Messinian Unit 1 are substantially concordant with the underlying succession and document continuous evolution from open marine (Tortonian) to progressively restricted (early Messinian) environments. Conversely, a sharp angular unconformity separates the coarse-grained conglomerates of Messinian Unit 2 from all underlying units, including the Hercynian basement complex and the pre-conglomerate Cenozoic sedimentary succession (Figs 3 and 4). The older Cenozoic rocks generally dip 30–50° eastward, and must have been rotated after Tortonian time, but prior to deposition of the Messinian fanglomerates. This geometric relationship demonstrates that deposition of the Messinian fanglomerates (Unit 2) cannot merely be the product of the lowering of the base level owing to the desiccation of the Mediterranean Sea, as also demonstrated by the fact that such conglomerates are not restricted to incised valleys but are also preserved in a structurally and topographically high position in the Calabrian orogenic wedge. In addition, this unconformity is widespread in the Mediterranean region (e.g. Decima and Wezel 1973; Fabri and Curzi 1979; Dondi 1985; Kastens *et al.* 1990;

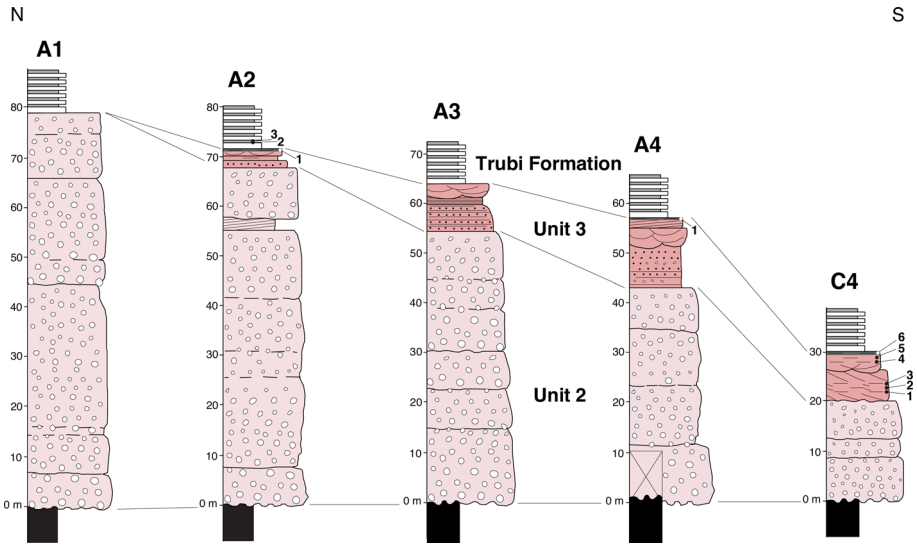

Fig. 6. Stratigraphic diagram of the upper Messinian post-evaporitic units of the Caulonia region. A1–A4 and C4 are the studied sections with the number and place of the analysed samples indicated by black and white dots (see Fig. 1 for location). Same legend as for Figure 5. Evaporites (Unit 1 of Figs 2 and 3) are absent in this region. Coarse-grained upper Messinian fanglomerates (Unit 2) overlie erosively the pelitic mélange of the Varicoloured clays (see Fig. 3). Upper Messinian shallow marine to transitional deposits of Unit 3 define a sedimentary prism pinching out toward the NW. Columns A1–A3 after Cavazza and DeCelles (1998).

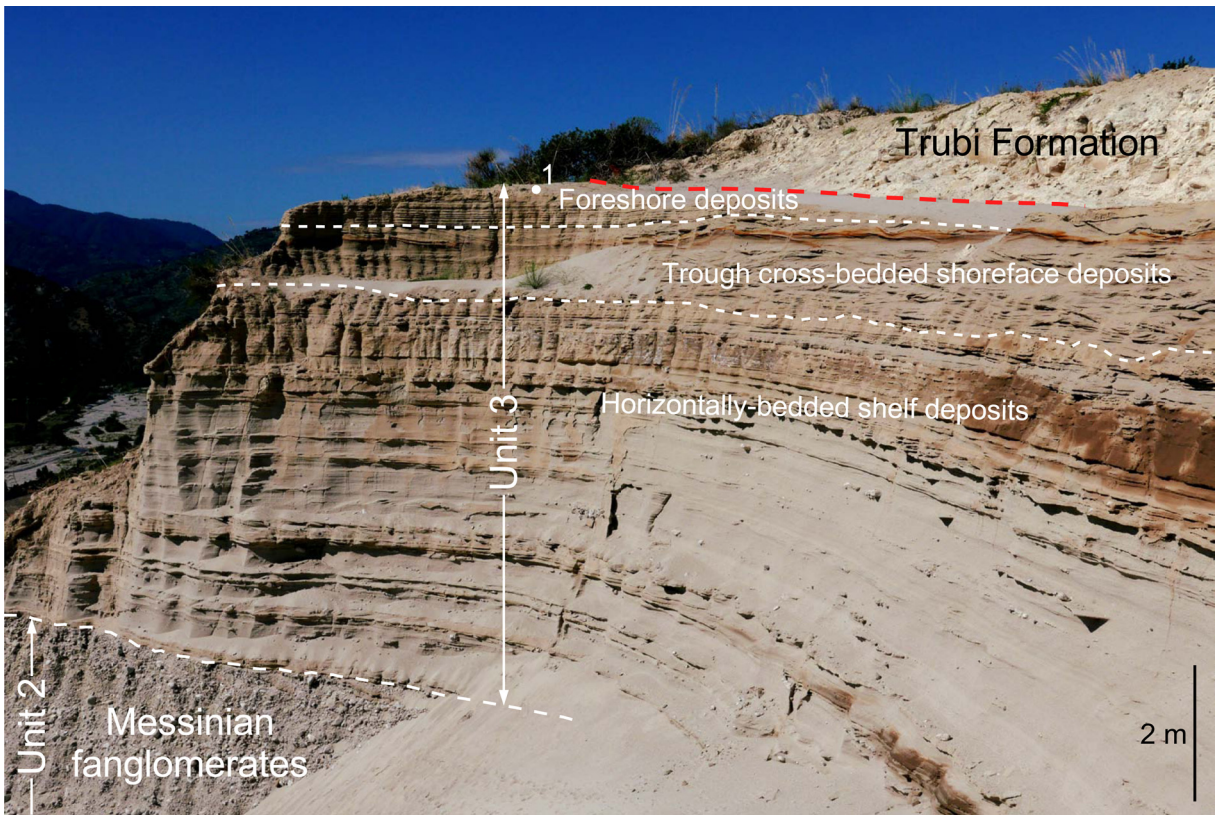

Fig. 7. Photograph of the upper part of section A4 (see Figs 1 and 5 for location) showing the topmost Unit 2, the entire Unit 3 and the lowermost Trubi Formation. White dot indicates studied sample. Upper Messinian Unit 3 forms a progradational parasequence from horizontally bedded shelf deposits (very coarse sandstone with microconglomerate stringers) through trough cross-bedded shoreface deposits (coarse to very coarse sandstones) to foreshore deposits (laminated, well-sorted coarse-to-medium sandstones).

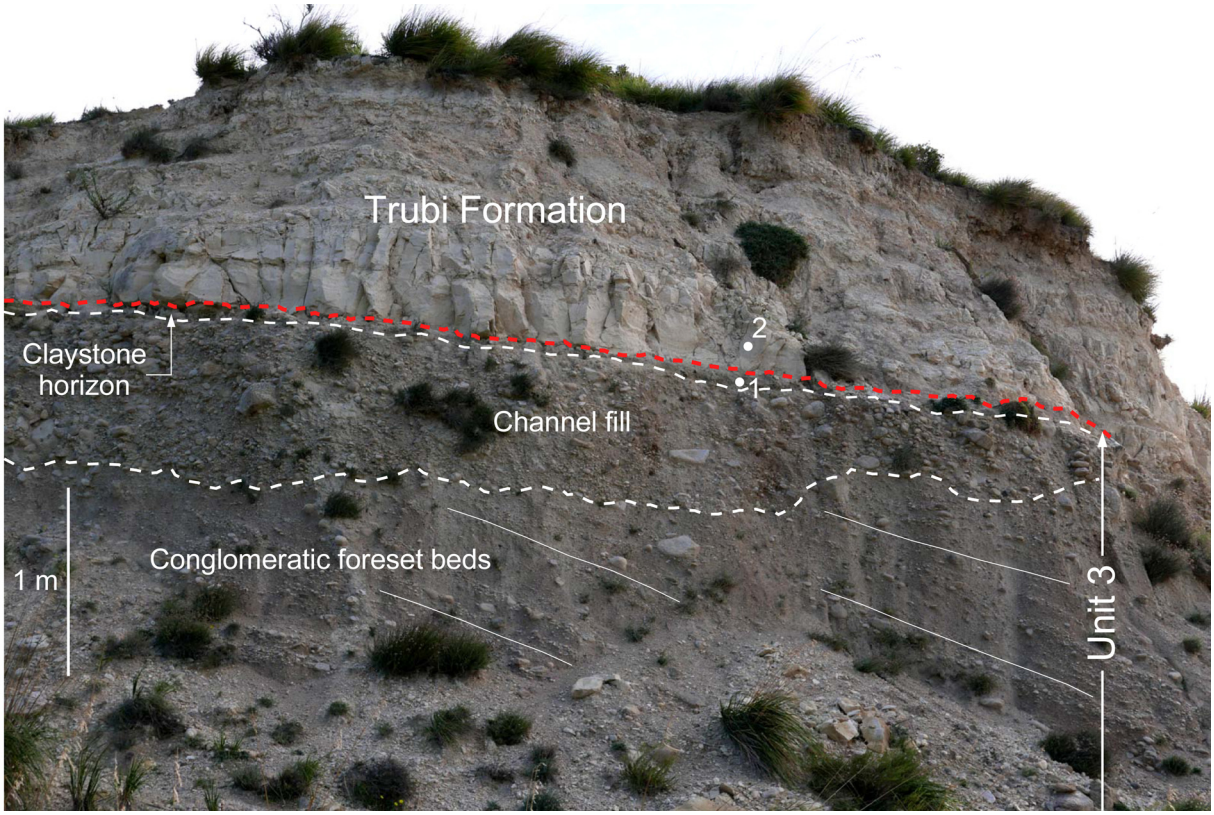

Fig. 8. Outcrop about 500 m north of the village of Careri exhibiting in its lower half a prograding braid-delta sequence. SE-dipping fluvial conglomerate foreset beds (delta-front deposits) of late Messinian Unit 2 are erosively overlain by channel-fill conglomerates (delta-plain deposits). The latter are in turn overlain by a thin claystone horizon closing Unit 3 and by the cyclic whitish grey calcilutites of the Zanclean Trubi Formation, which cover by onlap all older lithostratigraphic units in the region. White dots indicate studied samples.

Table 1. *Information on the six sampled locations*

Region	Location	Latitude (N)	Longitude (E)	Altitude (m)	Number of samples
Guardavalle	G3	38°30'28.97"	16°30'09.42"	265	3
	G5	38°28'38.79"	16°30'47.08"	110	2
Caulonia	A2	38°23'52.95"	16°26'07.12"	266	3
	A4	38°23'11.50"	16°26'11.70"	167	1
	C4	38°22'20.10"	16°25'18.60"	167	6
Careri		38°10'56.30"	16°06'56.00"	400	2

Butler *et al.* 1995; Riding *et al.* 1998; Braga *et al.* 2003), clearly pointing to intra-Messinian tectonic activity that significantly modified the regional physiography (Jolivet *et al.* 2006).

Micropalaeontology: methods and results

Seventeen samples were collected for micropalaeontological analyses near Guardavalle focusing on easily accessible clayey and silty facies within the upper part of Unit 3 and the lowermost layers of the Trubi Formation (Figs 5 and 6). Information on the locations sampled is provided in Table 1: most of the samples came from Unit 3 (location G3: samples 1–3; location G5: samples 1 and 2; location A2: sample 1; location A4: sample 1; location C4: samples 1–6; Careri : sample 1); a few samples came from the lowermost Trubi Formation (location A2: samples 2 and 3; Careri: sample 2). Careri (Fig. 8) is located outside the mapped area in Figure 1.

The methods used for microfossil extraction and identification were as follows:

- calcareous nannofossils: 2 g of sediment were used to prepare smear slides; the calcareous nannofossil analyses were performed using a light polarizing microscope at 1600× magnification; their taxonomic identification follows Perch-Nielsen (1985) and Young (1998);
- foraminifera: 10–15 g of sediment were disaggregated in a warm solution of sodium carbonate (Na_2CO_3); the residue was sieved at 50, 150 and 250 µm, and all the material was analysed and identified following Iaccarino and Premoli Silva (2007);
- dinoflagellate cysts: acid treatments were carried out using HCl, HF and again HCl on 10–15 g of sediment followed by concentration in $ZnCl_2$ (density 2.0) and sieving at 10 µm; a 50 µl volume of residue was mounted in glycerol and examined under a light microscope (magnification 1000×). Identification was based on the database of Williams *et al.* (2017).

Tables 2–4 list the results for calcareous nannofossils, planktonic foraminifera and dinoflagellate cysts, respectively.

Calcareous nannofossils

The samples from Unit 3 yielded a diversified calcareous nannofossil assemblage, evidence for an open marine environment (samples G3-1–3, G5-1 and -2, A2-1, A4-1, C4-1–6 and Careri-1; Figs 5 and 6). Table 2 lists the occurrence of some species of biostratigraphic significance: *Discoaster quinqueramus*, *Orthorhabdus* (ex *Triquetrorhabdulus*) *rugosus* and *Ceratolithus acutus* (Fig. 9). The highest occurrence (HO) of *D. quinqueramus* is suggested at about 5.53 Ma (Zeeden *et al.* 2013), but its extinction age in the Mediterranean has not been defined precisely. The lowest occurrence (LO) of *C. acutus* is indicated between 5.35 Ma (Raffi *et al.* 2006; Anthonissen and Ogg 2012) and 5.368 Ma (Zeeden *et al.* 2013). The two species were not recorded in the same samples, suggesting an age between 5.53 and 5.35 Ma for Unit 3. This is in agreement with the occurrence of *O. rugosus* (HO at 5.28 Ma: Raffi *et al.* 2006; Anthonissen and Ogg 2012). It should be noted that *Nicklithus amplificus* was recorded in a few samples from Unit 3 (Table 2) but must be considered as reworked because its HO is dated at about 5.94 Ma (Raffi *et al.* 2006; Anthonissen and Ogg 2012). The samples from the Trubi Formation (samples A2-2 and -3 and Careri-2; Figs 5 and 6) yielded a somewhat less diversified calcareous nannofossil assemblage, showing the occurrence of *O. rugosus* at location A2 (Table 2), consistent with the astronomical age of 5.30 Ma ascribed to the top of the first carbonate–marl precession cycle in the nearby Singa section in agreement with the base of the *Sphaeroidinellopsis* Acme (Van Couvering *et al.* 2000; Lirer *et al.* 2019). Figure 10 summarizes the calcareous nannofossil biostratigraphy and the inferred chronostratigraphy of Unit 3.

Planktonic foraminifera

Only three samples from the Trubi Formation from the location A2 and Careri (Fig. 6) yielded planktonic foraminifera that are on the whole, abundant (Table 3). This planktonic microfauna is evidence of normal marine conditions. Combined with the occurrence of *Sphaeroidinellopsis seminulina* and the absence of typical individuals of *Globorotalia margaritae*, its composition is consistent with the location of the samples in the lowermost Zanclean; that is, before the base of the *Sphaeroidinellopsis* Acme Zone (5.30 Ma; Lirer *et al.* 2019).

Dinoflagellate cysts

Six samples from Unit 3 (samples A4-1, C4-1 and -2 and C4-4–6; Fig. 6) yielded a dinoflagellate cyst flora (Table 4). The assemblage in sample A4-1 is dominated by *Lingulodinium machaerophorum* and *Homotryblium* sp., thus indicating coastal to lagoonal conditions. The assemblage from location C4 shows an interesting progression, from very poor (samples 1 and 2) to very rich (sample 6) in terms of diversity and the number of specimens. The latter, characterized by abundant cysts of *Impagidinium patulum* and *I. sphaericum* (Fig. 9), is evidence for full open marine conditions, whereas the underlying sample C4-4 rather points to a coastal environment. No dinoflagellate cyst originating from the Paratethys, constituting the Lago Mare biofacies as described by Popescu *et al.* (2015), was recorded in the samples studied here.

Overall, the clayey thin microfossiliferous beds of Unit 3 (Figs 5 and 6) may illustrate several successive minor sea-level rises, especially the uppermost one and its darker termination that immediately precedes the Trubi Formation.

Discussion

Previous studies have shown that the Messinian succession in southeastern Calabria was deposited in response to complex interactions between eustacy and tectonics (DeCelles and Cavazza 1995; Cavazza and DeCelles 1998). The abrupt vertical compositional change and angular unconformity between the evaporites of Unit 1 and the coarse-grained siliciclastic fanglomerates of Unit 2 were produced by intra-Messinian thrusting in the upper part of the

Table 2. *Occurrence of the calcareous nannofossils by location and sample*

Region:	Guardavalle					Caulonia										Careri	
Location:	G3			G5		A2			A4	C4							
Samples:	1*	2*	3*	1*	2*	1*	2†	3†	1*	1*	2*	3*	4*	5*	6*	1*	2†
Amaurolithus delicatus	x		x									x				x	x
Amaurolithus primus	x	x		x	x	x			x		x					x	
Calcidiscus leptoporus	x	x	x	x	x	x	x	x	x	x	x	x	x	x	x	x	x
Calcidiscus macintyrei	x	x	x	x	x	x	x	x	x	x	x	x	x	x	x	x	x
Ceratolithus acutus				x	x						x	x					
Coccolithus pelagicus	x	x	x	x	x	x	x	x	x	x	x	x	x	x	x	x	x
Discoaster asymmetricus				x	x						x	x		x	x		x
Discoaster berggrenii	x	x	x		x	x					x	x		x	x	x	x
Discoaster brouweri	x	x	x	x	x	x		x	x	x	x	x	x	x	x	x	x
Discoaster quinqueramus	x	x	x			x										x	
Discoaster surculus	x	x	x			x			x							x	x
Helicosphaera carteri	x	x	x	x	x	x	x	x	x	x	x	x	x	x	x	x	x
Helicosphaera sellii				x	x			x		x	x	x	x	x	x		x
Nicklithus amplificus			x													x	
Orthorhabdus rugosus	x	x				x	x									x	
Pontosphaera japonica	x	x	x	x	x	x	x	x	x	x	x	x	x	x	x	x	x
Pontosphaera multipora					x		x				x	x		x	x		
Reticulofenestra haquii	x	x	x	x	x	x	x	x	x	x	x	x	x	x	x	x	x
Reticulofenestra minuta	x	x	x	x	x	x	x	x	x	x	x	x	x	x	x	x	x
Reticulofenestra minutula	x	x	x	x	x	x	x	x	x	x	x	x	x	x	x	x	x
Reticulofenestra pseudoumbilicus	x	x	x	x	x	x	x	x	x	x	x	x	x	x	x	x	x
Rhabdosphaera clavigera	x	x	x			x										x	
Scyphosphaera spp.						x										x	
Sphenolithus abies	x	x	x				x	x		x			x				
Syracosphaera spp.		x	x			x										x	
Thoracosphaera spp.																	x
Reworked specimens	x	x	x	x	x	x	x	x	x	x	x	x	x	x	x	x	x

x, present.
*Sample from Unit 3.
†Sample from Trubi Formation.

Table 3. *Occurrence of the planktonic foraminifera by location and sample*

Region:	Caulonia		Careri
Location:	A2		
Samples:	2	3	2
Globigerina bulloides	x	x	x
Globigerina falconensis			x
Globigerinella obesa	x		x
Globigerinella siphonifera			x
Globigerinita glutinata			x
Globigerinita uvula			x
Globigerinoides bollii			x
Globigerinoides extremus	x	x	x
Globigerinoides quadrilobatus			x
Globigerinoides sacculifer			x
Globigerinoides trilobus	x		x
Globorotalia aff. *margaritae*			x
Globorotalia scitula	x		x
Globoturborotalita apertura		x	
Globoturborotalita decoraperta	x	x	x
Neogloboquadrina acostaensis sinistral	x		
Neogloboquadrina acostaensis dextral			x
Orbulina universa	x	x	x
Sphaeroidinellopsis seminulina	x		x

x, present. The three samples come from the Trubi Formation.

Calabrian orogenic prism. Reworking of these clastic deposits during the marine reflooding of the Mediterranean Basin produced the uppermost Messinian deposits of Unit 3, a coastal prism that was deposited by episodically prograding sandy shoreface systems (DeCelles and Cavazza 1992; Cavazza and DeCelles 1998). The subsequent general onlap of the pelagic oozes of the Trubi Formation at the Miocene–Pliocene boundary resulted from an additional sea-level rise, which drowned all pre-existing sedimentary deposits, somewhat reducing the land area and the terrigenous input to the basin, thereby promoting carbonate sedimentation in the basin (Butler *et al.* 1995; Bache *et al.* 2012).

Considering the large vertical distribution of samples containing marine microplankton (Figs 5 and 6), the micropalaeontological dataset presented in this paper confirms that Unit 3 was deposited in open marine conditions, as previously suggested by Cavazza and DeCelles (1998) based on purely stratigraphic and sedimentological grounds. Our results concerning the Calabrian Unit 3, the novelty of which is the evidence of marine microplankton including robust biostratigraphic markers (such as *Ceratolithus acutus* and *Orthorhabdus rugosus*), support the hypothesis that the marine reflooding that put an end to the MSC in the Mediterranean occurred significantly before the beginning of the Zanclean Stage corresponding formally to the base of the Trubi Formation.

The stratigraphy described by Karakitsios *et al.* (2017) in their Kalamaki East section on Zakynthos is particularly relevant to this discussion. In that area, a thin dark shale bed overlies a laminated greenish marly interval referred to as the Lago Mare biofacies above the Messinian Erosional Surface. Several samples from these two layers contain *Ceratolithus acutus* among other species of calcareous nannofossils and planktonic foraminifera. The dark shale bed is immediately overlain by the first carbonate layer of the Trubi Formation well dated by both micropalaeontological and magnetostratigraphic means (Karakitsios *et al.* 2017: sample KAL 134 in their fig. 16, table S1–S2). This context closely resembles the succession described by Bache *et al.* (2012) and Popescu *et al.* (2015) at the Zanclean GSSP (Eraclea Minoa, southern Sicily) comprising, from bottom to top, (1) the Messinian Discontinuity (the surface is considered to be due to marine reflooding), (2) the onlapping Arenazzolo silty Unit (including both Paratethyan and marine dinoflagellate cysts) topped by a thin dark clayey bed, and finally (3) the Trubi Formation. Accordingly, a comparison of the latest Messinian–earliest Zanclean succession of the classic locations in southern Calabria and southern Sicily is needed because they probably both belong to a similar palaeogeographical context along the front of the Calabrian accretionary wedge corresponding to relatively coastal conditions.

Calabria versus Sicily latest Messinian–earliest Zanclean succession

The comparison focuses mainly on Calabrian Unit 3 (Cavazza and DeCelles 1998) and the Sicilian Arenazzolo Unit (Ogniben 1957; Bache *et al.* 2012; Popescu *et al.* 2015); that is, the units located stratigraphically between the Messinian evaporites at the bottom and the Trubi Formation at the top. In Calabria, the contact between Unit 3 and Unit 2 (fanglomerate) is sharp (Fig. 7) and can be interpreted as a ravinement surface delimiting the base of the sedimentary prism of Unit 3 (Figs 5 and 6; Cavazza and DeCelles 1998). In several places (Fig. 6), a clayey dark bed of variable thickness ends Unit 3, the uppermost 3–5 cm of which are darker and are in sharp colour contrast with the whitish first carbonate bed of the Trubi Formation (Figs 10 and 13). As argued above, this dark layer, observed in the Caulonia region (locations A4 and C4) and at

Table 4. *Results of the dinoflagellate cyst analyses detailed by location and sample, including the suggested palaeoenvironment*

Region:	Caulonia					
Location:	C4					A4
Samples:	1	2	4	5	6	1
Achomosphaera andalousiensis						1
Brigantedinium sp.		1				
Cyst of *Pentapharsodinium dalei*			1		1	
Edwardsiella sexispinosa			1			
Homotryblium sp.			7		4	22
Hystrichokolpoma sp.			1			
Hystrichokolpoma rigaudiae			1			1
Impagidinium aculeatum					7	1
*Impagidinium patulum**	2		13	9	80	2
Impagidinium sp.			1	2	6	2
*Impagidinium sphaericum**				1	20	
Impagidinium strialatum						1
Invertocysta tabulata			1	1		1
Lingulodinium machaerophorum†	1		12	2	10	67
Melitasphaeridium choanophorum			3		2	3
Nematosphaeropsis labyrinthus				1	2	
Nematosphaeropsis lattivitatus					6	
Operculodinium centrocarpum‡		1	4	1	2	7
Operculodinium janduchenei			3	1	8	6
Polysphaeridium zoharyi			1			2
Quinquecuspis concreta						1
Reticulatosphaera actinocoronata					1	1
Selenopemphix nephroides						7
Spiniferites bulloideus						1
Spiniferites falcipedius			1			
Spiniferites hyperacanthus			1			1
Spiniferites mirabilis	1		1			
Spiniferites ramosus			1	1		3
Spiniferites sp. (marine)			2	2		7
Reworked individuals			5	3		11

Samples are from Unit 3.
*Open marine species.
†Coastal to lagoonal species.
‡Coastal species.

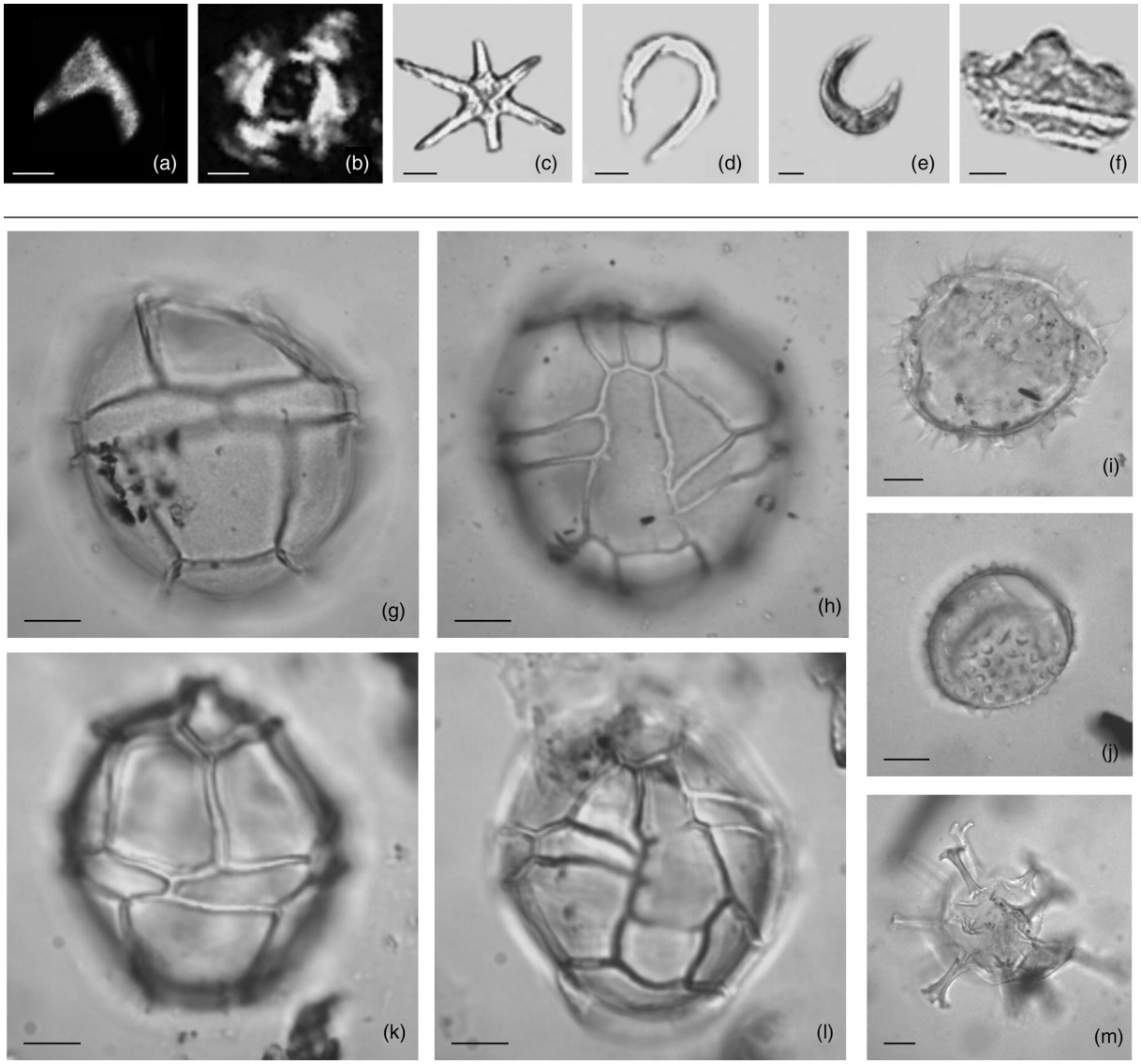

Fig. 9. Photographs of some specimens of calcareous nannofossils and dinoflagellate cysts. (**a**–**f**) Calcareous nannofossils in polarized light (scale bar represents 5 μm). (**a**) *Ceratolithus acutus* Gartner and Bukry 1974, crossed Nicols, location C4, sample 2. (**b**) *Reticulofenestra pseudoumbilicus* (Gartner 1967) Gartner 1969, crossed Nicols, location G3, sample 1. (**c**) *Discoaster brouweri* (Tan Sin Hok 1927) Bramlette and Riedel 1954, parallel Nicols, location C4, sample 1. (**d**) *Amaurolithus delicatus* Gartner and Bukry 1975, parallel Nicols, location G3, sample 1. (**e**) *Amaurolithus primus* (Bukry and Percival 1971) Gartner and Bukry 1975, parallel Nicols, location C4, sample 2. (**f**) *Orthorhabdus* (ex. *Triquetrorhabdulus*) *rugosus* (Bramlette and Wilcoxon 1967) Young and Brown 2014, parallel Nicols, location G3, sample 1. (**g**–**m**) Dinoflagellate cysts in natural light from location C4, sample 6 (scale bar represents 10 μm). (**g**, **h**) *Impagidinium patulum* (Wall 1967) Stover and Evitt 1978: (**g**) dorsal view of ventral surface; (**h**) ventral view. (**i**) *Lingulodinium machaerophorum* (Deflandre and Cookson 1955) Wall 1967, ventral view of ventral surface, mid focus. (**j**) *Operculodinium janduchenei* Head *et al.* 1989, dorsal view of dorsal surface, mid focus. (**k**, **l**) *Impagidinium sphaericum* (Wall 1967) Lentin and Williams 1981: (**k**) dorsal view of ventral surface; (**l**) ventral view. (**m**) *Homotryblium* sp. Davey and Williams 1966, right lateral view, mid focus.

Careri (Figs 6, 8 and 10), rich in marine microplankton (Tables 2 and 4), results from a sea-level rise and represents maximum flooding. At Eraclea Minoa in Sicily, the Arenazzolo and Trubi formations can be traced for a few hundred metres. Here, a well-marked discontinuity was evidenced at the base of the Arenazzolo Unit, called the 'Messinian Discontinuity' by Popescu *et al.* (2009, 2015) and Bache *et al.* (2012). In southern Calabria, this discontinuity marks a clear separation between units 2 and 3. Its smooth morphology and wide regional extent lead us to interpret this surface as resulting from transgressive ravinement (i.e. a wave-cut surface; see modern and past examples described by Bache *et al.* 2012). At Eraclea Minoa, this surface marks the base of an assemblage of inner-to-outer-shelf dinoflagellate cysts also containing Paratethyan species (Bache *et al.* 2012). The sedimentary gap has been interpreted as corresponding to the second, paroxysmal, step of the MSC (Clauzon *et al.* 1996; Bache *et al.* 2012). In this paper, we therefore call this discontinuity a 'transgressive ravinement surface' (TRS) (Fig. 13) as defined by Catuneanu and Zecchin (2013). The overlying Arenazzolo Unit is thus suggested as marking the marine reflooding of the Mediterranean Basin, as also shown by a marine, although relatively poor, calcareous nannofossil assemblage (Bache *et al.* 2012), in line with earlier suggestions (Brolsma 1975, 1976). Bache *et al.* (2012) proposed that marine reflooding occurred at 5.46 Ma, based on a tentative cyclostratigraphy. This age is consistent with the LO of *Discoaster quinqueramus* and the FO of *Ceratolithus acutus* (Fig. 10) for the reflooding event recorded in Calabria. This event must be regarded as a sudden marked rise of the Mediterranean sea-level, which was estimated at *c.* 500 m by Bache *et al.* (2012) (Fig. 13). In addition, the Arenazzolo Unit corresponds to the third Lago Mare episode (LM3: high sea-level Paratethys–Mediterranean exchanges; Clauzon *et al.* 2005) closely linked to marine reflooding (for details see Popescu

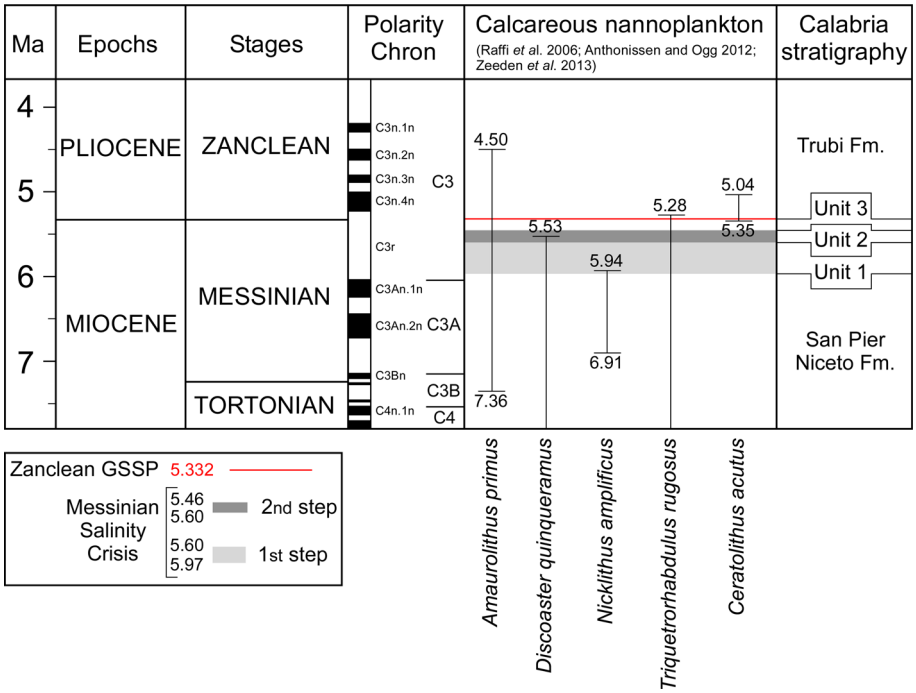

Fig. 10. Chrono-biostratigraphic chart of key calcareous nannofossil species with reference to the two steps of the Messinian Salinity Crisis (Clauzon *et al.* 1996) and the Zanclean GSSP (Van Couvering *et al.* 2000). Involvement in the Calabria stratigraphy. Polarity Chron is from Hilgen *et al.* (2012).

et al. 2015). Like the Calabrian Unit 3, the Arenazzolo Unit ends with a 50 cm thick clayey layer, the uppermost centimetres of which are darker (Fig. 13), that we interpret as a condensed interval representing a maximum flooding event.

Palaeoenvironmental and palaeogeographical inferences

The proposed chronostratigraphic correlation of the Sicilian Arenazzolo Unit with the Calabrian Unit 3 (Fig. 13) and their comparison leads us to palaeoenvironmental interpretations that can be integrated in up-to-date knowledge of palaeogeography.

The latest Messinian pre-Trubi siliciclastic units of Sicily and Calabria have a consistent stratigraphic position but vary in thickness and sedimentary facies. For example, Calabrian Unit 3 comprises palaeoenvironments ranging from fully marine to continental (DeCelles and Cavazza 1992, 1995; Cavazza and DeCelles 1998) and varies in thickness from 0 to 52 m (Figs 5 and 6). The extensive outcrops of Unit 3 three-dimensionally delineate a ribbon-shaped sedimentary body, elongated along the strike of the Messinian depositional system, virtually parallel to the present-day coastline. This depositional system developed over a rugged palaeotopography (hence the lateral variations in facies, thickness and stacking pattern) and prograded into a deep body of water (hence a wide accommodation space). Conversely, the Arenazzolo Unit appears to be rather uniformly characterized by brackish to marine palaeoenvironments (Bache *et al.* 2012) and its thickness is limited and somewhat more uniform over the entire Sicilian Caltanissetta Basin (Decima and Wezel 1973). This suggests a limited accommodation space; that is, shallower water than in Calabria. The calcareous nannofossil assemblage leads to the same conclusion, being more abundant and diversified in Unit 3 than in the Arenazzolo Unit (Bache *et al.* 2012). Deeper conditions offshore South Calabria are supported by palaeogeographical reconstructions showing the proximity of the Ionian Basin, where evaporites were deposited during the second step of the MSC (Fig. 12; Jolivet *et al.* 2006; Haq *et al.* 2020; Manzi *et al.* 2020). Evaporites of the Caltanissetta Basin have long been considered to belong to the deep central Mediterranean basins (i.e. deposited during the second step of the MSC). Clauzon *et al.* (1996) and Bertini *et al.* (1998) placed them in the first step of the MSC. Today, there is a wide consensus for ascribing them to a peripheral basin, probably deeper than the more internal peri-Mediterranean basins such as Sorbas (Clauzon *et al.* 1996; CIESM 2008; Roveri *et al.* 2014). An onshore–offshore study in Tunisia supports the two-step MSC scenario (Clauzon *et al.* 1996): peripheral evaporites of the first step show a gypsum–anhydrite–halite succession (borehole Carthage 1; Fig. 12) similar in both thickness and structure to that of

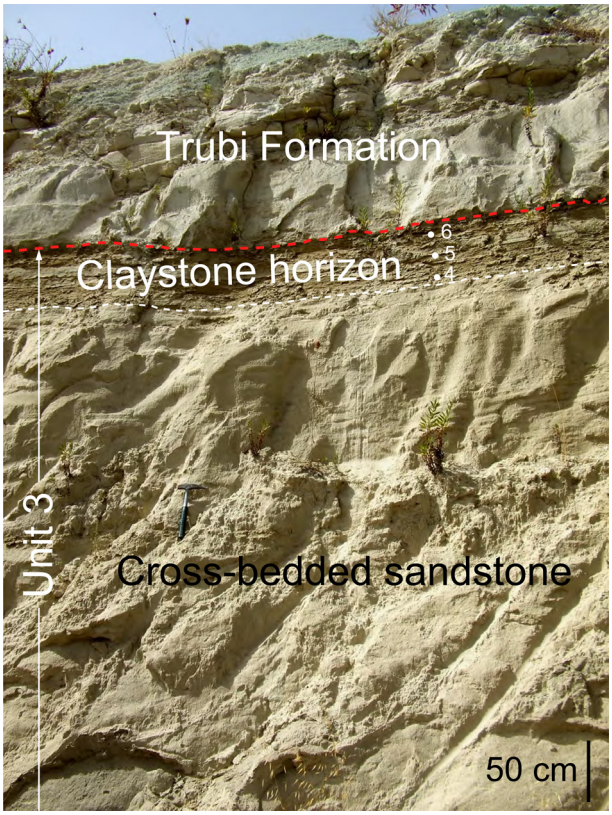

Fig. 11. View of the claystone horizon ending Unit 3 covered by the Trubi Formation in locality C4 (see Figs 1 and 6 for location). White dots indicate studied samples.

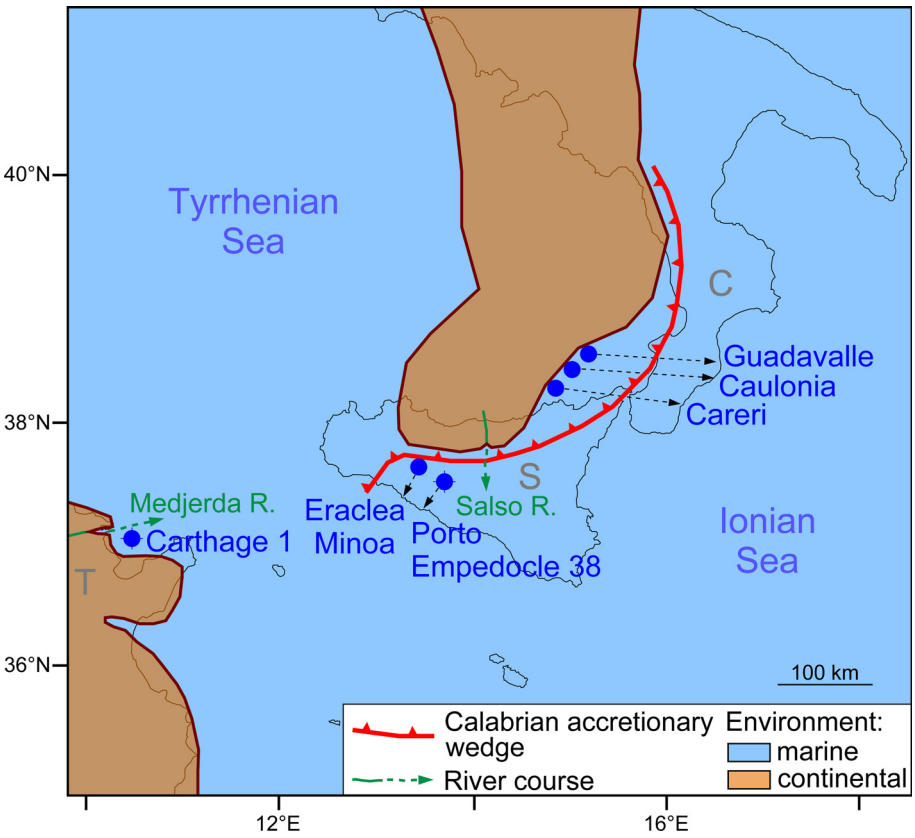

Fig. 12. Palaeogeographical sketch at time of deposition of Calabrian Unit 3 and Sicilian Arenazzolo Unit at 5.46 Ma, based on maps published by Bache *et al.* (2012), Henriquet *et al.* (2020) and Manzi *et al.* (2020). The shift of the considered locations from 5.46 Ma is indicated by arrows with dotted black lines in the present geographical outline. C, Calabria; S, Sicily; T, Tunisia.

Sicily (borehole Porto Empedocle 38; Fig. 12), cut by the deep fluvial canyon of the Medjerda River (Fig. 12) demonstrating the second step of the MSC (El Euch-El Koundi *et al.* 2009). This evidence implies that, at that time, the Sicily–Tunisia marine domain should be considered a peripheral basin including some deeper parts (El Euch-El Koundi *et al.* 2009). A similar conclusion was proposed by Micallef *et al.* (2019) for the Sicily–Tunisia domain, which, during the second step of the MSC, was separated from the Ionian Basin by the eroded Malta Escarpment. The peripheral status of the Sicilian Basin is also supported by the erosional cutting caused by the Salso River at the northern edge of the basin (Fig. 12; El Euch-El Koundi *et al.* 2009; Maniscalco *et al.* 2019). We conclude that the latest Messinian successions of southern Calabria and Sicily, although deposited in bathymetrically rather different conditions, likewise recorded the pre-Zanclean reflooding of the Mediterranean Basin.

Revisited significance of some geological formations

Three Lago Mare episodes, mainly characterized by the influx of Paratethyan dinoflagellates (i.e. transported by surface waters), have been identified during the latest Messinian–earliest Zanclean time interval (Clauzon *et al.* 2005; Popescu *et al.* 2009, 2015; Do Couto *et al.* 2014). The first and the third episodes (LM1 and LM3),

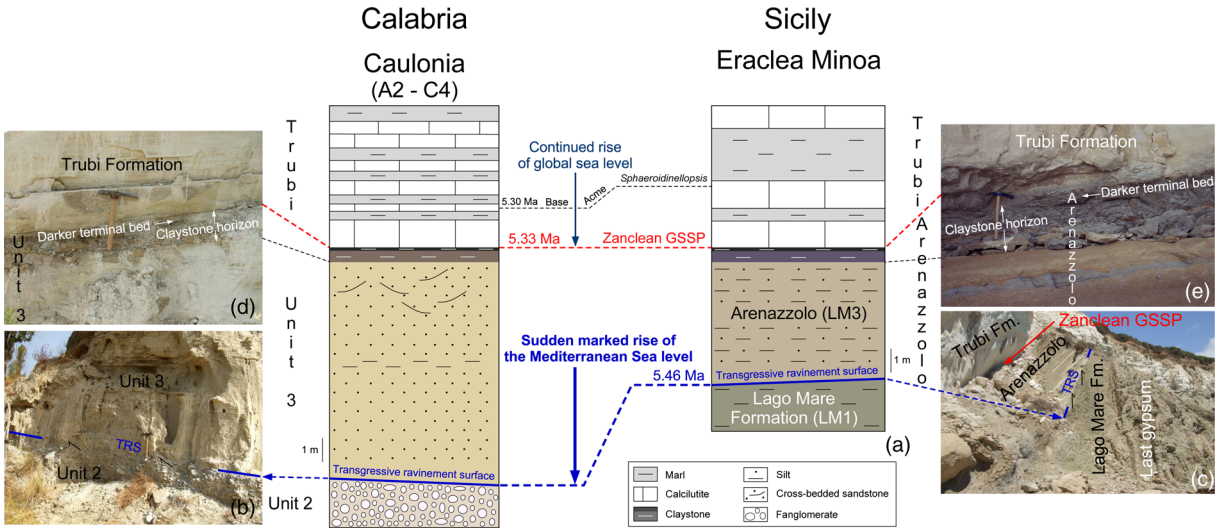

Fig. 13. Comparison of the latest Messinian–earliest Zanclean succession between Calabria and Sicily. (**a**) Lithological successions and chronostratigraphic relationships; (**b**) transgressive ravinement surface (TRS) marking the contact of Unit 3 over Unit 2 in the Caulonia region (location A2; Fig. 6); (**c**) Eraclea Minoa, Sicily (section of the Zanclean GSSP): TRS marking the unconformable contact of the Arenazzolo Unit over the Lago Mare Formation; (**d**) detail of the topmost Unit 3 in the Caulonia region (location C4; Fig. 6); (**e**) topmost Arenazzolo Unit at Eraclea Minoa.

recorded in both peripheral and central basins, occurred respectively at the end of the first MSC step and during the post-crisis marine reflooding and were caused by high sea-level exchanges between the Mediterranean and Paratethys. The second episode (LM2), recorded only in the central basins in both the western and eastern Mediterranean, occurred immediately after the peak of the MSC and is interpreted as resulting from an overflow from the perched Aegean realm that pooled Paratethyan waters (Popescu *et al.* 2015). The Eraclea Minoa stratigraphic section records the LM1 and LM3 episodes (Fig. 13; for details see Popescu *et al.* 2009, 2015; Bache *et al.* 2012), the latter being located within the Arenazzolo Unit. As a consequence, we expected to find Paratethyan dinoflagellate cysts in the Calabrian Unit 3, but our search was unsuccessful. The absence of Paratethyan dinoflagellate cysts in the south Calabria Unit 3 could be explained by the high-energy sediment input from the continent resulting in thinner clayey deposits compared with thick coarser clastic deposits (Figs 5 and 6).

The integration of pre-existing stratigraphic, sedimentological and palaeontological data from the latest Messinian Unit 3 of southeastern Calabria and the correlative Arenazzolo Unit in Sicily confirms that fully marine conditions were re-established in the Mediterranean Basin well before the initial deposition of the Trubi Formation, traditionally considered as the first marine unit after the end of the MSC (e.g. Van Couvering *et al.* 2000, and references therein). Earlier reports of the occurrence of pre-Trubi marine microplankton (Brolsma 1975, 1976; Londeix *et al.* 2007) were dismissed, possibly because they challenged the widely accepted scenario of the 'Zanclean deluge'; that is, a virtually synchronous flooding of the Mediterranean Basin that gained acceptance within the scientific community. This 'deluge' is thought to be marked by the base of the Trubi Formation, providing a convenient datum for the formal establishment of the base of the Pliocene. However, in the last few years, a growing body of evidence points to a more complex sequence of events, with at least two stages in the refilling of the Mediterranean Basin (Bache *et al.* 2012). Based on micropalaeontological data, the present study validates the hypothesis that the uppermost Messinian marine deposits below the Trubi Formation represent complete reflooding of the Mediterranean Basin followed by further sea-level rise recorded by the Trubi Formation driven by glacioeustacy (Miller *et al.* 2011; Gorini *et al.* 2014).

Conclusion

In southern Calabria, a coastal sedimentary prism (Unit 3) characterizes the latest Messinian and is overlain by the Zanclean Trubi Formation, traditionally considered as the re-establishment of fully marine conditions in the Mediterranean Basin following the Messinian Salinity Crisis. Analyses of physical stratigraphy and sedimentary facies previously evidenced that Unit 3 marks a transgressive event ending with a maximum flooding condensed interval just below the highstand recorded by the Trubi Formation. Calcareous nannofossils and dinoflagellate cysts found in the present study show that this unit is fully marine. We thus conclude that the marine reflooding of the Mediterranean Basin that ended the MSC occurred significantly before the beginning of the Zanclean Stage. The Sicilian Arenazzolo Unit is time equivalent to the Calabrian Unit 3. Sharp lithological breaks do not correspond to the most important environmental changes, such as the passage from a terrigenous succession to carbonate sedimentation probably promoted by continuous sea-level rise. The Trubi Formation is not the expression of the post-MSC marine reflooding but denotes only a glacio-eustatic rise in sea-level. The marine reflooding significantly predates the Zanclean GSSP. An age of 5.46 Ma is thus conceivable for the end of the Messinian Salinity Crisis, more than 100 kyr before the beginning of the Zanclean.

Acknowledgements Portions of this study developed from past collaboration between W. Cavazza and P. G. DeCelles and from the geological mapping of several students at the University of Bologna (M. Dall'Olmo, S. Gangemi, M. Macchiarola, L. Zanarini and A. Zanutta). N. Loget and J. Van Den Driessche participated in a preliminary reconnaissance. D. Do Couto reviewed an earlier version of this paper. W. B. F. Ryan and two anonymous referees reviewed the paper and contributed significantly to its improvement.

Author contributions **SMP**: formal analysis (equal), methodology (equal), project administration (lead), writing – original draft (equal), writing – review & editing (equal); **WC**: conceptualization (lead), funding acquisition (equal), investigation (equal), writing – original draft (equal), writing – review & editing (equal); **JPS**: investigation (equal), writing – original draft (equal), writing – review & editing (equal); **MCMD**: formal analysis (equal), methodology (equal), writing – review & editing (equal); **NB**: formal analysis (equal), methodology (equal), writing – review & editing (equal); **CG**: funding acquisition (equal), writing – review & editing (equal)

Funding Funding for this research was provided over the years by ISTeP, the GRI South Tethys (University P. & M. Curie – TOTAL), the TerMex Program (MISTRALS), CNR, MIUR, NATO and the University of Bologna.

Data availability All data generated or analysed during this study are included in this article.

Scientific editing by Stephen Lokier

References

Adams, C.G., Benson, R.H., Kidd, R.B., Ryan, W.B.F. and Wright, R.C. 1977. The Messinian salinity crisis and evidence of late Miocene eustatic changes in the world ocean. *Nature*, **269**, 383–386, https://doi.org/10.1038/269383a0

Aguirre, J. and Sánchez-Almazo, I.M. 2004. The Messinian post-evaporitic deposits of the Gafares area (Almería–Níjar basin, SE Spain). A new view of the 'Lago-Mare' facies. *Sedimentary Geology*, **168**, 71–95, https://doi.org/10.1016/j.sedgeo.2004.03.004

Alvarez, W., Cocozza, T. and Wezel, F.C. 1974. Fragmentation of the Alpine orogenic belt by microplate dispersal. *Nature*, **248**, 309–314, https://doi.org/10.1038/248309a0

Amodio Morelli, L., Bonardi, G. *et al.* 1976. L'arco calabro-peloritano nell'orogene appenninico-maghrebide. *Memorie della Società Geologica Italiana*, **17**, 1–60.

Anthonissen, D.E. and Ogg, J.G. 2012. Cenozoic and Cretaceous biochronology of planktonic foraminifera and calcareous nannofossils. *In*: Gradstein, F.M., Ogg, J.G., Schmitz, M.D. and Ogg, G.M. (eds) *The Geologic Time Scale 2012*. Elsevier, Amsterdam, 1083–1127.

Bache, F., Popescu, S.-M. *et al.* 2012. A two-step process for the reflooding of the Mediterranean after the Messinian Salinity Crisis. *Basin Research*, **24**, 125–153, https://doi.org/10.1111/j.1365-2117.2011.00521.x

Bache, F., Gargani, J. *et al.* 2015. Messinian evaporite deposition during sea level rise in the Gulf of Lions (Western Mediterranean). *Marine and Petroleum Geology*, **66**, 262–277, https://doi.org/10.1016/j.marpetgeo.2014.12.013

Bertini, A., Londeix, L. *et al.* 1998. Paleobiological evidence of depositional conditions in the Salt Member, Gessoso–Solfifera Formation (Messinian, Upper Miocene) of Sicily. *Micropaleontology*, **44**, 413–433, https://doi.org/10.2307/1486042

Bonardi, G., Giunta, G., Perrone, V., Russo, M., Zuppetta, A. and Ciampo, G. 1980. Osservazioni sull'evoluzione dell'arco calabro-peloritano nel Miocene inferiore: la Formazione di Stilo–Capo d'Orlando. *Bolletino della Società Geologica Italiana*, **99**, 365–393.

Bonardi, G., Cavazza, W., Perrone, V. and Rossi, S. 2001. Calabria–Peloritani terrane and northern Ionian Sea. *In*: Vai, G.B. and Martini, I.P. (eds) *Anatomy of an Orogen: the Apennines and Adjacent Mediterranean Basins*. Kluwer, Dordrecht, 287–306.

Braga, J.C., Martín, J. and Quesada, C. 2003. Patterns and average rates of late Neogene–Recent uplift of the Betic Cordillera, SE Spain. *Geomorphology*, **50**, 3–26, https://doi.org/10.1016/S0169-555X(02)00205-2

Bramlette, M.N. and Riedel, W.R. 1954. Stratigraphic value of discoasters and some other microfossils related to Recent coccolithophores. *Journal of Paleontology*, **28**, 385–403.

Bramlette, M.N. and Wilcoxon, J.A. 1967. Middle Tertiary calcareous nannoplankton of the Cipero section, Trinidad, W.I. *Tulane Studies in Geology and Paleontology.* **5**, 93–131.

Brolsma, M.J. 1975. Lithostratigraphy and foraminiferal assemblages of the Miocene–Pliocene transitional strata of Capo Rossello and Eraclea Minoa (Sicily, Italy). *Proceedings of the Koninklijke Nederlandse Akademie Van Wetenschappen, Series B*, **78**, 341–380.

Brolsma, M.J. 1976. Discussion on the arguments concerning the palaeoenvironmental interpretation of the Arenazzolo in Capo Rossello and Eraclea Minoa (S. Sicily, Italy). *Memoria della Società Geologica Italiana*, **16**, 153–157.

Bukry, D. and Percival, S.F. 1971. New Tertiary calcareous nannofossils. *Tulane Studies in Geology and Paleontology*, **8**, 123–146.

Butler, R.W.H., Lickorish, W.H., Grasso, M., Pedley, H.M. and Ramberti, L. 1995. Tectonics and sequence stratigraphy in Messinian basins, Sicily: constraints on the initiation and termination of the Mediterranean salinity crisis. *Geological Society of America Bulletin*, **107**, 425–439, https://doi.org/10.1130/0016-7606(1995)107<0425:TASSIM>2.3.CO;2

Carnevale, G., Longinelli, A., Caputo, D., Barbieri, M. and Landini, W. 2008. Did the Mediterranean marine reflooding precede the Mio–Pliocene boundary? Paleontological and geochemical evidence from upper Messinian sequences of Tuscany, Italy. *Palaeogeography, Palaeoclimatology, Palaeoecology*, **257**, 81–105, https://doi.org/10.1016/j.palaeo.2007.09.005

Catuneanu, O. and Zecchin, M. 2013. High-resolution sequence stratigraphy of clastic shelves II: controls on sequence development. *Marine and Petroleum Geology*, **39**, 26–38, https://doi.org/10.1016/j.marpetgeo.2012.08.010

Cavazza, W. 1989. Detrital modes and provenance of the Stilo–Capo d'Orlando Formation (Miocene), southern Italy. *Sedimentology*, **36**, 1077–1090, https://doi.org/10.1111/j.1365-3091.1989.tb01543.x

Cavazza, W. and Barone, M. 2010. Large-scale sedimentary recycling of tectonic mélange in a forearc setting: the Ionian basin (Oligocene–Quaternary, southern Italy). *Geological Society of America Bulletin*, **122**, 1932–1949, https://doi.org/10.1130/B30177.1

Cavazza, W. and DeCelles, P.G. 1993. Miocene submarine canyons and associated sedimentary facies in southeastern Calabria, southern Italy. *Geological Society of America Bulletin*, **105**, 1297–1309, https://doi.org/10.1130/0016-7606(1993)105<1297:GOAMSC>2.3.CO;2

Cavazza, W. and DeCelles, P.G. 1998. Upper Messinian siliciclastic rocks in southeastern Calabria (southern Italy): paleotectonic and eustatic implications for the evolution of the central Mediterranean region. *Tectonophysics*, **298**, 223–241, https://doi.org/10.1016/S0040-1951(98)00186-3

Cavazza, W., Blenkinsop, J., DeCelles, P., Patterson, R.T. and Reinhardt, E.D. 1997. Stratigrafia e sedimentologia della sequenza sedimentaria oligocenico-quaternaria del bacino calabro-ionico di avanarco. *Bollettino della Società Geologica Italiana*, **116**, 51–77.

Cavazza, W., Roure, F. and Ziegler, P.A. 2004. The Mediterranean area and the surrounding regions: active processes, remnants of former Tethyan oceans and related thrustbelts. *In*: Cavazza, W., Roure, F., Spakman, Stampfli, G.M. and Ziegler, P.A. (eds) *The TRANSMED Atlas: the Mediterranean Region from Crust to Mantle*. Springer, Berlin, 1–29.

Channell, J.E.T., Rio, D. and Thunell, R.C. 1988. Miocene/Pliocene boundary magnestostratigraphy at Capo Spartivento, Calabria, Italy. *Geology*, **16**, 1096–1099, https://doi.org/10.1130/0091-7613(1988)016<1096:MPBMAC>2.3.CO;2

CIESM. 2008. Executive Summary. *CIESM Workshop Monographs*, **33**, 7–28.

Cita, M.B. 1973. Inventory of biostratigraphical findings and problems. *Initial Reports of the Deep Sea Drilling Project*, **13**, 1045–1073, doi:10.2973/dsdp.proc.13.140.1973

Cita, M.B., Wright, R.C., Ryan, W.B.F. and Longinelli, A. 1978. Messinian paleoenvironments. *Initial Reports of the Deep Sea Drilling Project,* **42**, 1003–1035, https://doi.org/10.2973/dsdp.proc.42-1.153.1978

Clauzon, G., Suc, J.-P., Gautier, F., Berger, A. and Loutre, M.-F. 1996. Alternate interpretation of the Messinian salinity crisis: controversy resolved? *Geology*, **24**, 363–366, https://doi.org/10.1130/0091-7613(1996)024<0363:AIOTMS>2.3.CO;2

Clauzon, G., Suc, J.-P., Popescu, S.-M., Marunteanu, M., Rubino, J.-L., Marinescu, F. and Melinte, M.C. 2005. Influence of the Mediterranean sea-level changes over the Dacic Basin (Eastern Paratethys) in the Late Neogene. The Mediterranean Lago Mare facies deciphered. *Basin Research*, **17**, 437–462, https://doi.org/10.1111/j.1365-2117.2005.00269.x

Clauzon, G., Suc, J.-P. *et al.* 2015. New insights on the Sorbas Basin (SE Spain): the onshore reference of the Messinian Salinity Crisis. *Marine and Petroleum Geology*, **66**, 71–100, https://doi.org/10.1016/j.marpetgeo.2015.02.016

Cohen, K.M., Finney, S.C., Gibbard, P.L. and Fan, J.-X. 2020. International Chronostratigraphic Chart, http://www.stratigraphy.org/ICSchart/ChronostratChart2020-03.pdf

Cornée, J.-J., Ferrandini, M. *et al.* 2006. The late Messinian erosional surface and the subsequent reflooding in the Mediterranean: new insights from the Melilla–Nador basin (Morocco). *Palaeogeography, Palaeoclimatology, Palaeoecology*, **230**, 129–154, https://doi.org/10.1016/j.palaeo.2005.07.011

Critelli, S., Muto, F. and Tripodi, V. 2015*a*. *Geological Map of Italy, 1:50,000 Scale, Sheet 630 Bovalino*. Geological Survey of Italy, Rome.

Critelli, S., Muto, F. and Tripodi, V. 2015*b*. *Geological Map of Italy, 1:50,000 Scale, Sheet 590 Taurianova*. Geological Survey of Italy, Rome.

Davey, R.J. and Williams, G.L. 1966. V. The genus Hystrichosphaeridium and its allies. In: Davey, R.J., Downie, C., Sarjeant, W.A.S. and Williams, G.L. (eds) *Studies on Mesozoic and Cainozoic dinoflagellate cysts*. British Museum (Natural History). Geology, Bulletin, Supplement, **3**, 53–106.

De Astis, G., Ventura, G. and Vilardo, G. 2003. Geodynamic significance of the Aeolian volcanism (southern Tyrrhenian Sea, Italy) in light of structural, seismological, and geochemical data. *Tectonics*, **22**, 1040–1057, https://doi.org/10.1029/2003TC001506

DeCelles, P.G. and Cavazza, W. 1992. Constraints on the formation of Pliocene hummocky cross-stratification in Calabria (southern Italy) from consideration of hydraulic and dispersive equivalence, grain-flow theory and suspended-load fallout rate. *Journal of Sedimentary Petrology*, **62**, 555–568, https://doi.org/10.1306/D426795B-2B26-11D7-8648000102C1865D

DeCelles, P. and Cavazza, W. 1995. Upper Messinian fanglomerates in eastern Calabria (southern Italy): response to microplate migration and Mediterranean sea-level changes. *Geology*, **23**, 775–778, https://doi.org/10.1130/0091-7613(1995)023<0775:UMCICS>2.3.CO;2

Decima, A. 1964. Ostracodi del genere *Cyprideis* Jones del Neogene e del Quaternario italiani. *Palaeontographia Italica*, **57**, 81–133.

Decima, A. and Wezel, F.C. 1973. Late Miocene evaporites of the central Sicilian Basin. *Initial Reports of the Deep Sea Drilling Project*, **13**, 1234–1241, doi:10.2973/dsdp.proc.13.144-1.1973

Decima, A., McKenzie, J.A. and Schreiber, B.C. 1988. The origin of 'evaporative' limestones: an example from the Messinian of Sicily (Italy). *Journal of Sedimentary Petrology*, **58**, 256–272, https://doi.org/10.1306/212F8D6E-2B24-11D7-8648000102C1865D

Deflandre, G. and Cookson, I.C. 1955. Fossil microplankton from Australian Late Mesozoic and Tertiary sediments. *Australian Journal of Marine and Freshwater Research*, **6**, 242–313.

Dercourt, J., Zonenshain, L.P. *et al.* 1985. Présentation de 9 cartes paléogéographiques au 1/20.000.000^{e} s'étendant de l'Atlantique au Pamir pour la période du Lias à l'Actuel. *Bulletin de la Société Géologique de France, Série 8,* **1**, 637–652.

Dewey, J.F., Helman, M.L., Turco, E., Hutton, D.W.H. and Knott, S.D. 1989. Kinematics of the Western Mediterranean. *Geological Society, London, Special Publications*, **45**, 265–283, https://doi.org/10.1144/GSL.SP.1989.045.01.15

Do Couto, D., Popescu, S.-M. *et al.* 2014. Lago Mare and the Messinian Salinity Crisis: evidences from the Alboran Sea (S. Spain). *Marine and Petroleum Geology*, **52**, 57–76, https://doi.org/10.1016/j.marpetgeo.2014.01.018

Dondi, L. 1985. Pianura Padana: paleogeografia dall'Oligocene superior al Pleistocene. Atti del Convegno Regionale di Cartografia di Bologna, 1985, Regione Emilia–Romagna, 76–101.

El Euch-El Koundi, N., Ferry, S. *et al.* 2009. Messinian deposits and erosion in northern Tunisia: inferences on Strait of Sicily during the Messinian Salinity Crisis. *Terra Nova*, **21**, 41–48, https://doi.org/10.1111/j.1365-3121.2008.00852.x

Fabri, A. and Curzi, P. 1979. The Messinian of the Tyrrhenian Sea: seismic evidence and dynamic implications. *Giornale di Geologia*, **43**, 215–248.

Gartner, S. 1967. Calcareous nannofossils from Neogene of Trinidad, Jamaica, and Gulf of Mexico. *University of Kansas Paleontological Contributions, Papers,* **29**, 1–7.

Gartner, S. 1969. Correlation of Neogene planktonic foraminifera and calcareous nannofossil zones. *Transactions of the Gulf-Coast Association of Geological Societies*, **19**, 585–599.

Gartner, S. and Bukry, D. 1974. Ceratolithus acutus Gartner and Bukry n. sp. and Ceratolithus amplificus Bukry and Percival - nomenclatural clarification. *Tulane Studies in Geology and Paleontology*, **11**, 115–118.

Gartner, S. and Bukry, D. 1975. Morphology and phylogeny of the coccolithophycean family Ceratolithaceae. *Journal of Research of the U.S. Geological Survey*, **3**, 451–465.

Gautier, F., Clauzon, G., Suc, J.-P., Cravatte, J. and Violanti, D. 1994. Age et durée de la crise de salinité messinienne. *Comptes-Rendus de l'Académie des Sciences de Paris, Série 2*, **318**, 1103–1109.

Glangeaud, L., Alinat, J., Polvèche, J., Guillaume, A. and Leenhardt, O. 1966. Grandes structures de la mer Ligure, leur evolution et leurs relations avec les chaînes continentales. *Bulletin de la Société géologique de France*, **7**, 921–937.

Gorini, C., Haq, B.U., dos Reis, A.T., Silva, C.G., Cruz, A., Soares, E. and Grangeon, D. 2014. Late Neogene sequence stratigraphic evolution of the Foz do Amazonas Basin, Brazil. *Terra Nova*, **26**, 179–185, https://doi.org/10.1111/ter.12083

Gueguen, E., Doglioni, C. and Fernandez, M. 1998. On the post-25 Ma geodynamic evolution of the western Mediterranean. *Tectonophysics*, **298**, 259–269, https://doi.org/10.1016/S0040-1951(98)00189-9

Guido, A., Jacob, J., Gautret, P., Laggoum-Défarge, Mastandrea, A. and Russo, F. 2007. Molecular fossils and other organic markers as palaeoenvironmental indicators of the Messinian Calcare di Base Formation: normal *versus* stressed marine deposition (Rossano Basin, northern Calabria, Italy). *Palaeogeography, Palaeoclimatology, Palaeoecology*, **255**, 265–283, https://doi.org/10.1016/j.palaeo.2007.07.015

Haq, B., Gorini, C., Baur, J., Moneron, J. and Rubino, J.-L. 2020. Deep Mediterranean's Messinian evaporite giant: how much salt? *Global and Planetary Change*, **184**, 103052, https://doi.org/10.1016/j.gloplacha.2019.103052

Head, M.J., Norris, G. and Mudie, P.J. 1989. New species of dinocysts and a new species of acritarch from the upper Miocene and lowermost Pliocene, ODP Leg 105, Site 646, Labrador Sea. Proceedings of the Ocean Drilling Program, *Scientific Results*, **105**, 453–466, https://doi.org/10.2973/odp.proc.sr.105.136.1989

Henriquet, M., Dominguez, S., Barreca, G., Malavieille, J. and Monaco, C. 2020. Structural and tectono-stratigraphic review of the Sicilian orogen and new insights from analogue modeling. *Earth-Science Reviews*, **208**, 103257, https://doi.org/10.1016/j.earscirev.2020.103257

Hilgen, F.J. 1987. Sedimentary rhythms and high-resolution chronostratigraphic correlations in the Mediterranean Pliocene. *Newsletters on Stratigraphy*, **17**, 109–127, https://doi.org/10.1127/nos/17/1987/109

Hilgen, F.J. 1991. Extension of the astronomically calibrated (polarity) time scale to the Miocene/Pliocene boundary. *Earth and Planetary Science Letters*, **107**, 349–368, https://doi.org/10.1016/0012-821X(91)90082-S

Hilgen, F.J. and Langereis, C.G. 1993. A critical re-evaluation of the Miocene/Pliocene boundary as defined in the Mediterranean. *Earth and Planetary Science Letters*, **118**, 167–179, https://doi.org/10.1016/0012-821X(93)90166-7

Hilgen, F.J., Lourens, L.J. and Van Dam, J.A. 2012. The Neogene Period. *In*: Gradstein, F., Ogg, J., Schmitz, M. and Ogg, G. (eds) *The Geological Time Scale 2012*. Elsevier, Amsterdam, 923–978.

Hsü, K.J. 1972. Origin of Saline Giants: a critical review after the discovery of the Mediterranean evaporite. *Earth-Science Reviews*, **8**, 371–396, https://doi.org/10.1016/0012-8252(72)90062-1

Hsü, K.J., Cita, M.B. and Ryan, W.B.F. 1973*a*. The origin of the Mediterranean evaporites. *Initial Reports of the Deep Sea Drilling Project*, **13**, 1203–1231, https://doi.org/10.2973/dsdp.proc.13.143.1973

Hsü, K.J., Ryan, W.B.F. and Cita, M. 1973*b*. Late Miocene desiccation of the Mediterranean. *Nature*, **242**, 240–244, https://doi.org/10.1038/242240a0

Iaccarino, S. and Bossio, A. 1999. Paleoenvironment of uppermost Messinian sequences in the Western Mediterranean (Sites 974, 975, and 978). *Proceedings of the Ocean Drilling Program, Scientific Results*, **161**, 529–541, https://doi.org/10.2973/odp.proc.sr.161.246.1999.

Iaccarino, S.M. and Premoli Silva, I. 2007. Practical manual of Neogene planktonic foraminifera. *In*: Biolzi, M., Iaccarino, S.M., Turco, E., Checconi, A. and Rettori, R. (eds) *International School on Planktonic Foraminifera*. Università degli Studi di Perugia, 1–142.

Jolivet, L. and Faccenna, C. 2000. Mediterranean extension and the Africa–Eurasia collision. *Tectonics*, **19**, 1095–1106, https://doi.org/10.1029/2000TC900018

Jolivet, L., Augier, R., Robin, C., Suc, J.-P. and Rouchy, J.M. 2006. Lithospheric-scale geodynamic context of the Messinian salinity crisis. *Sedimentary Geology*, **188–189**, 9–33, https://doi.org/10.1016/j.sedgeo.2006.02.004

Karakitsios, V., Roveri, M. *et al.* 2017. A record of the Messinian salinity crisis in the eastern Ionian tectonically active domain (Greece, eastern Mediterranean). *Basin Research*, **29**, 203–233, https://doi.org/10.1111/bre.12173

Kastens, K.A., Mascle, J. *et al.* (eds) 1990. *Tyrrhenian Sea*. Proceedings of the Ocean Drilling Program. Scientific Results, **107**, https://doi.org/10.2973/odp.proc.sr.107.1990

Krijgsman, W., Hilgen, F.J., Raffi, I., Sierro, F.J. and Wilson, D.S. 1999. Chronology, causes and progression of the Messinian salinity crisis. *Nature*, **400**, 652–655, https://doi.org/10.1038/23231

Krijgsman, W., Fortuin, A.R., Hilgen, F.J. and Sierro, F.J. 2001. Astrochronology for the Messinian Sorbas basin (SE Spain) and orbital (precessional) forcing for evaporite cyclicity. *Sedimentary Geology*, **140**, 43–60, https://doi.org/10.1016/S0037-0738(00)00171-8

Krijgsman, W., Capella, W. *et al.* 2018. The Gibraltar Corridor: Watergate of the Messinian Salinity Crisis. *Marine Geology*, **403**, 238–246, https://doi.org/10.1016/j.margeo.2018.06.008

Lentin, J.K. and Williams, G.L. 1981. Fossil dinoflagellates: index to genera and species, 1981 edition. *Bedford Institute of Oceanography, Report Series*, **BI-R-81-12**.

Lirer, F., Foresi, L.M. *et al.* 2019. Mediterranean Neogene planktonic foraminifer biozonation and biochronology. *Earth-Science Reviews*, **196**, 102869, https://doi.org/10.1016/j.earscirev.2019.05.013

Londeix, L., Benzakour, M., Suc, J.-P. and Turon, J.-L. 2007. Messinian palaeoenvironments and hydrology in Sicily (Italy): the dinoflagellate cyst record. *Geobios*, **40**, 233–250, https://doi.org/10.1016/j.geobios.2006.12.001

Malinverno, A. and Ryan, W.B.F. 1986. Extension in the Tyrrhenian Sea and shortening in the Apennines as result of arc migration driven by sinking of the lithosphere. *Tectonics*, **5**, 227–245, https://doi.org/10.1029/TC005i002p00227

Maniscalco, R., Casciano, C.I., Distefano, S., Grossi, F. and Di Stefano, A. 2019. Facies analysis in the Second Cycle Messinian evaporites predating the early Pliocene reflooding: the Balza Soletta section (Corvillo Basin, central Sicily). *Italian Journal of Geosciences*, **138**, 301–316, https://doi.org/10.3301/IJG.2019.06

Manzi, V., Lugli, S., Roveri, M., Schreiber, B.C. and Gennari, R. 2011. The Messinian 'Calcare di Base' (Sicily, Italy) revisited. *Geological Society of America Bulletin*, **123**, 347–370, https://doi.org/10.1130/B30262.1

Manzi, V., Gennari, R., Hilgen, F., Krijgsman, W., Lugli, S., Roveri, M. and Sierro, F.J. 2013. Age refinement of the Messinian salinity crisis onset in the Mediterranean. *Terra Nova*, **25**, 315–322, https://doi.org/10.1111/ter.12038

Manzi, V., Argnani, A., Corcagnani, A., Lugli, S. and Roveri, M. 2020. The Messinian salinity crisis in the Adriatic foredeep: evolution of the largest evaporitic marginal basin in the Mediterranean. *Marine and Petroleum Geology*, **115**, 104288, https://doi.org/10.1016/j.marpetgeo.2020.104288

Melinte-Dobrinescu, M.C., Suc, J.-P. *et al.* 2009. The Messinian Salinity Crisis in the Dardanelles region. Chronostratigraphic constraints. *Palaeogeography, Palaeoclimatology, Palaeoecology*, **278**, 24–39, https://doi.org/10.1016/j.palaeo.2009.04.009

Micallef, A., Camerlenghi, A. *et al.* 2019. Geomorphic evolution of the Malta Escarpment and implications for the Messinian evaporative drawdown in the eastern Mediterranean Sea. *Geomorphology*, **327**, 264–283, https://doi.org/10.1016/j.geomorph.2018.11.012

Miller, K.G., Mountain, G.S., Wright, J.D. and Browning, J.V. 2011. A 180-million-year record of sea level and ice volume variations from continental margin and deep-sea isotopic records. *Oceanography*, **24**, 40–53, https://doi.org/10.5670/oceanog.2011.26

Montadert, L., Sancho, J., Fail, J.P., Debyser, J. and Winnock, E. 1970. De l'âge tertiaire de la série salifère responsable des structures diapiriques en Méditerranée Occidentale (Nord-Est des Baléares). *Comptes Rendus de l'Académie des Sciences*, **271**, 812–815.

Ogniben, L. 1957. Petrografia della Serie Solfifera Siciliana e considerazioni geologiche relative. *Memorie Descrittive della Carta Geologica d'Italia*, **33**, 1–275.

Patterson, R.T., Blenkinsop, J. and Cavazza, W. 1995. Planktic foraminiferal biostratigraphy and $^{87}Sr/^{86}Sr$ isotopic stratigraphy of the Oligocene-to-Pleistocene sedimentary sequence in the southeastern Calabrian microplate, southern Italy. *Journal of Paleontology*, **69**, 7–20, https://doi.org/10.1017/S0022336000026871

Pellen, R., Popescu, S.-M. *et al.* 2017. The Apennine foredeep (Italy) during the latest Messinian: Lago Mare reflects competing brackish and marine conditions based on calcareous nannofossils and dinoflagellate cysts. *Geobios*, **50**, 237–257, https://doi.org/10.1016/j.geobios.2017.04.004

Perch-Nielsen, K. 1985. Cenozoic calcareous nannofossils. *In*: Bolli, H.M., Saunders, J.B. and Perch-Nielsen, K. (eds) *Plankton Stratigraphy*. Cambridge University Press, Cambridge, 427–554.

Popescu, S.-M., Dalesme, F. *et al.* 2009. *Galeacysta etrusca* complex, dinoflagellate cyst marker of Paratethyan influxes into the Mediterranean Sea before and after the peak of the Messinian Salinity Crisis. *Palynology*, **33**, 105–134, https://doi.org/10.2113/gspalynol.33.2.105

Popescu, S.-M., Dalibard, M. *et al.* 2015. Lago Mare episodes around the Messinian–Zanclean boundary in the deep southwestern Mediterranean. *Marine and Petroleum Geology*, **66**, 55–70, https://doi.org/10.1016/j.marpetgeo.2015.04.002

Raffi, I., Backman, J., Fornaciari, E., Pälike, H., Rio, D., Lourens, L. and Hilgen, F. 2006. A review of calcareous nannofossil astrobiochronology encompassing the past 25 million years. *Quaternary Science Reviews*, **25**, 3113–3137, https://doi.org/10.1016/j.quascirev.2006.07.007

Riding, R., Braga, J.C., Martín, J.M. and Sánchez-Almazo, I. 1998. Mediterranean Messinian Salinity Crisis: constraints from a coeval marginal basin, Sorbas, southeastern Spain. *Marine Geology*, **146**, 1–20, https://doi.org/10.1016/S0025-3227(97)00136-9

Roveri, M., Flecker, R. *et al.* 2014. The Messinian Salinity Crisis: past and future of a great challenge for marine sciences. *Marine Geology*, **352**, 25–50, https://doi.org/10.1016/j.margeo.2014.02.002

Ruggieri, G. 1967. The Miocene and later evolution of the Mediterranean Sea. *Systematics Association, Special Publications*, **7**, 283–290.

Ryan, W.B.F. 2009. Decoding the Mediterranean salinity crisis. *Sedimentology*, **56**, 95–136, https://doi.org/10.1111/j.1365-3091.2008.01031.x

Selli, R. 1954. Il Bacino del Metauro. *Giornale di Geologia*, **24**, 1–294.

Selli, R. 1960. Il Messiniano Mayer-Eymar 1867. Proposta di un neostratotipo. *Giornale di Geologia*, **28**, 1–33.

Soria, J.M., Caracuel, J.E., Corbí, H., Dinarès-Turell, J., Lancis, C., Tent-Manclús, J.E. and Yébenes, A. 2008. The Bajo Segura Basin (SE Spain): implications for the Messinian salinity crisis in the Mediterranean margins. *Stratigraphy*, **5**, 257–263.

Spakman, W. and Wortel, R. 2004. A tomographic view on western Mediterranean geodynamics. *In*: Cavazza, W., Roure, F., Spakman, W., Stampfli, G.M. and Ziegler, P.A. (eds) *The TRANSMED Atlas: the Mediterranean Region From Crust to Mantle*. Springer, Berlin, 31–52.

Sternai, P., Caricchi, L., Garcia-Castellanos, D., Jolivet, L., Sheldrake, T.E. and Castelltort, S. 2017. Magmatic pulse driven by sea-level changes associated with the Messinian salinity crisis. *Nature Geoscience*, **10**, 783–787, https://doi.org/10.1038/ngeo3032

Stover, L.E. and Evitt, W.R. 1978. Analyses of pre-Pleistocene organic-walled dinoflagellates. *Stanford University Publications, Geological Sciences*, 15.

Suc, J.-P., Bache, F., Çağatay, M.N. and Csato, I. 2015. Messinian events and hydrocarbon exploration in the Mediterranean: an introduction. *Marine and Petroleum Geology*, **66**, 1–5, https://doi.org/10.1016/j.marpetgeo.2015.05.006

Tan Sin Hok 1927. Discoasteridae incertae sedis. Proceedings of the Koninklijke Nederlandse Akademie van Wetenschappen. *Section Science*, **30**, 411–419.

Thunnell, R.C., Williams, D.F. and Howell, M. 1987. Atlantic–Mediterranean water exchange during the late Neogene. *Paleoceanography*, **2**, 661–678, https://doi.org/10.1029/PA002i006p00661

Tortorici, D.L., Monaco, C., Tansi, C. and Cocina, O. 1995. Recent and active tectonics in the Calabrian arc (Southern Italy). *Tectonophysics*, **243**, 37–55, https://doi.org/10.1016/0040-1951(94)00190-K

Vai, G.B. and Ricci-Lucchi, F. 1977. Algal crusts, autochthonous and clastic gypsum in a cannibalistic evaporite basin: a case history from the Messinian of northern Apennines. *Sedimentology*, **24**, 211–244, https://doi.org/10.1111/j.1365-3091.1977.tb00255.x

Van Couvering, J.A., Castradori, D., Cita, M.B., Hilgen, F.J. and Rio, D. 2000. The base of the Zanclean Stage and of the Pliocene Series. *Episodes*, **23**, 179–187, https://doi.org/10.18814/epiiugs/2000/v23i3/005

Van Dijk, J.P. 1992. *Late Neogene Fore-arc Basin Evolution in the Calabrian Arc (Central Mediterranean): Tectonic Sequence Stratigraphy and Dynamic Geohistory*. PhD thesis, University of Utrecht.

Wall, D. 1967. Fossil microplankton in deep-sea cores from the Caribbean Sea. *Palaeontology*, **10**, 95–123.

Williams, G.L., Fensome, R.A. and MacRae, R.A. 2017. DINOFLAJ3, American Association of Stratigraphic Palynologists, Data Series no. 2, http://dinoflaj.smu.ca/dinoflaj3

Young, J.R. 1998. Chapter 8: Neogene. *In*: Bown, P.R. (ed.) *Calcareous Nannofossils Biostratigraphy*. *British Micropaleontological Society Publications Series*. Kluwer, Dordrecht, 225–265.

Young, J.R. and Bown, P.R. 2014. Some emendments to calcareous nannoplankton taxonomy. *Journal of Nannoplankton Research* **33**, 39–46.

Zeeden, C., Hilgen, F., Westerhold, T., Lourens, L., Röhl, U. and Bickert, T. 2013. Revised Miocene splice, astronomical tuning and calcareous plankton biochronology of ODP Site 926 between 5 and 14.4 Ma. *Palaeogeography, Palaeoclimatology, Palaeoecology*, **369**, 430–451, https://doi.org/10.1016/j.palaeo.2012.11.009

Zijderveld, J.D.A., Zachariasse, W.J., Verhallen, P.J.J.M. and Hilgen, F.J. 1986. The age of the Miocene–Pliocene boundary. *Newsletters on Stratigraphy*, **16**, 169–181, https://doi.org/10.1127/nos/16/1986/169